University of Liège

Study of an active mass damper

Linear control systems

Bastien Hoffmann (20161283)
Maxime Meurisse (20161278)
Valentin Vermeylen (20162864)

Master in Civil Engineering

Academic year 2019-2020

Contents

1 Control problem

1.1 Choice of the topic

The chosen topic is : **Active mass damper**.

1.2 Context

The current engineering prowesses allow us to construct buildings higher and higher. These constructions are subject to various disturbances (mainly wind, but also earthquakes) that make them oscillate. They turn into giant pendulum and swing from left to right, sometimes moving several meters at the top ! [1]

To reduce these oscillations, one uses a passive system, called *tuned mass damper*, which consists in concealing a tuned and harmonic oscillator at the top of the tower. It is coupled to its movement and oscillates in phase opposition to recover the kinetic energy of the tower and thus reduces the oscillations. [2]

An active version of this system exists : the *active mass damper*. It relies on the same principle as the tuned mass damper but it is equipped with sensors and actuators to measure the oscillations of its environment and, via an algorithm, generates a force acting on the mass to reduce, or totally remove, these oscillations. [3]

The field of study of this project focuses on the active mass damper systems used to reduce the oscillations caused by the **wind** on **tall** buildings.

1.3 Control problem diagram

The diagram of our control problem is shown in figure 1.

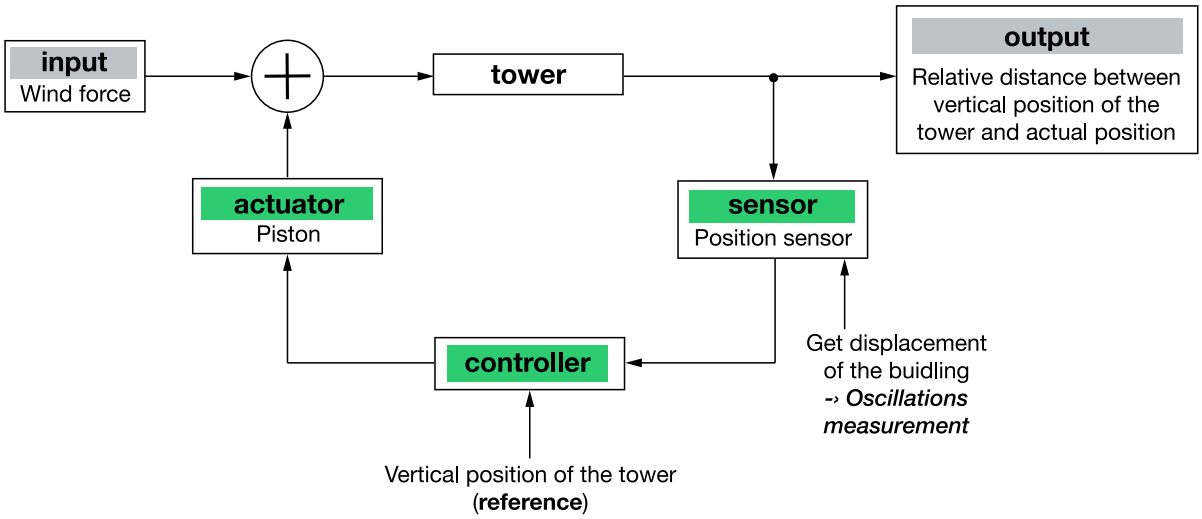

Figure 1 – Control problem diagram of the active mass damper for tall buildings

1.4 Control problem description

- **Utility of the controller** : the controller (the algorithm) allows the system (the tower) to be active, *i.e.* to measure the oscillations to which it is subjected and to cancel it. Thanks to a piston connected to the controller, the mass can move and reduce, or even eliminate totally, the oscillations.
- **System to be controlled** : the tower (and the position of the tower is the signal)
- **Inputs of the system** : wind force acting on the tower (uncontrollable) and force acting on the mass damper (controllable).
- **Outputs of the system** : the relative distance between the vertical position and the displacement of the tower.
- **Reference** : the vertical position of the tower.
- **Actuators** : piston to move the mass that reduces the oscillations.
- **Constraints and limitations** : to simplify our system, we consider a tower 200 m high, perfectly vertical when it undergoes no disturbance. The only disturbance on this tower is the force of the wind. The wind, ranging from a few tens of km/h to a hundred km/h, can swing the tower from a few millimeters to several centimeters. Additional constraints are given in section 2.

1.5 Open loop system diagram

The detailed schematic of the open loop studied system is shown in figure 2.

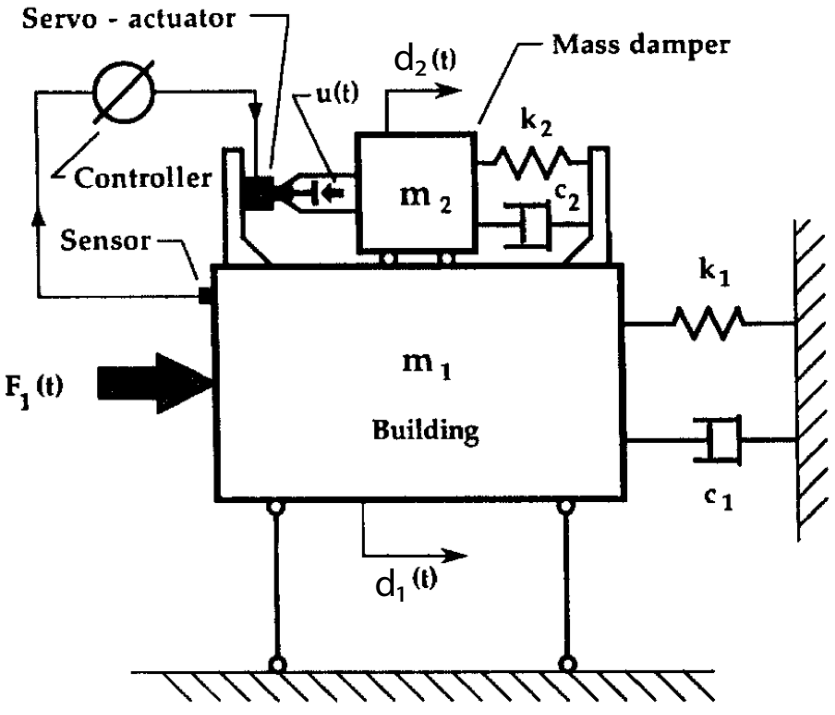

Figure 2 – Detailed schematic of the open loop studied system [3]

The building is represented by the mass m_1 and its natural resistance to movement is simulated by the spring k_1 and the damper c_1.

The mass damper is represented by the mass m_2 and its movement is simulated by the spring k_2 and the damper c_2.

The force $F_1(t)$ represents the wind force (uncontrollable) on the building.

The force $u(t)$ represents the force applied on the mass damper by the controller (controllable).

At first, the system is studied without a control mechanism. The controllable input $u(t)$ will therefore be 0 for all our simulations in the following section.

2 State-space representation

2.1 Open loop model description

Input vector U and state vector X are given by :

$$U = \begin{pmatrix} F_1 \\ u \end{pmatrix} \qquad\qquad X = \begin{pmatrix} d_1 \\ \dot{d}_1 \\ d_2 \\ \dot{d}_2 \end{pmatrix}$$

2.1.1 Inputs

- $F_1(t)$, the force of the wind (uncontrollable), between 500 and 1500 kN (which corresponds to a wind speed of 10 to 15 $\mathrm{m\,s^{-1}}$ on our building).
- $u(t)$, the force applied on the mass damper (controllable), in the order of 500 kN.

The sensor considered is a measurement of the horizontal position of the top of the building relatively to the vertical position $d_1 = 0$.

The actuator provides a force on the mass of the dampener ($u(t)$), sets it in motion.

2.1.2 Outputs

$y = d_1(t)$ the relative position of the building with respect to the vertical position.

2.1.3 States

- $x_1 = d_1$, as described above, ranging from a few millimeters to a few centimeters.
- $x_2 = \dot{d}_1$, the speed of the building, ranging from about 0 to 5 $\mathrm{m\,s^{-1}}$.
- $x_3 = d_2$, the relative displacement of the mass damper, ranging from about 0 to 5 m.
- $x_4 = \dot{d}_2$, the speed of the mass damper, ranging from about 0 to 10 $\mathrm{m\,s^{-1}}$.

2.1.4 Output law

The output is one of the states : $y = x_1$.

2.1.5 Update law

The update law is given by [3] :

$$\begin{cases} m_1\ddot{d}_1 + c_1\dot{d}_1 + k_1 d_1 = c_2\dot{z} + k_2 z + F_1(t) - u(t) \\ m_2\ddot{z} + c_2\dot{z} + k_2 z = -m_2\ddot{d}_1 + u(t) \end{cases}$$

with $z = d_2 - d_1$.

2.2 State-space model

The system is **linear**. The ABCD matrices can be easily derived.

$$A = \begin{pmatrix} 0 & 1 & 0 & 0 \\ \frac{-k_1-k_2}{m_1} & \frac{-c_2-c_1}{m_1} & \frac{k_2}{m_1} & \frac{c_2}{m_1} \\ 0 & 0 & 0 & 1 \\ \frac{k_2}{m_2} & \frac{c_2}{m_2} & \frac{-k_2}{m_2} & \frac{-c_2}{m_2} \end{pmatrix} \quad B = \begin{pmatrix} 0 & 0 \\ \frac{1}{m_1} & -\frac{1}{m_1} \\ 0 & 0 \\ 0 & \frac{1}{m_2} \end{pmatrix}$$

$$C = \begin{pmatrix} 1 & 0 & 0 & 0 \end{pmatrix} \quad D = \begin{pmatrix} 0 & 0 \end{pmatrix}$$

2.3 Constraints, limitations and numerical choice of parameter values

To model and study the system, a series of constraints have to be defined, as well as assumptions and limitations.

2.3.1 Basic system constraints

The basic modeling constraints of our system are presented in table 1.

Building	height of 200 m, width of 30 m movement along a single axis (horizontal)
Mass	no friction between m_1 and m_2

Table 1 – Basic system constraints

2.3.2 Constraints on signals

The constraints on the different signals of our system[1] are presented in table 2.

[1] Given by our common sense and computations for the uncontrollable input. The maximum value of the controllable input corresponds to an acceleration of $1.6g$.

Reference	a few millimeters or even a few centimeters at most (we expect it to remain 0mm)
Controllable input	in the order of 500 kN
Uncontrollable input	between 500 and 1500 kN
Output	from a few millimeters to a few centimeters (we don't want it to exceed 1m)

Table 2 – Constraints on signals

2.3.3 Numerical values for simulations

To simulate the system (without control mechanism), a series of numerical values, presented in table 3[2] were chosen.

Mass	$m_1 = 1 \times 10^7\,\text{kg}$	$m_2 = 3 \times 10^4\,\text{kg}$
Spring	$k_1 \approx 4 \times 10^8\,\text{N/m}$	$k_2 = 10^5\,\text{N/m}$
Damper	$c_1 \approx 1.3 \times 10^6\,\text{Ns/m}$	$c_2 = 10^4\,\text{Ns/m}$
Wind	$F_{max} = 810\,000\,\text{N}$	

Table 3 – Numerical values of the system

The stiffness and viscosity values for the building were obtained using the formulas :

$$k_1 = (2\pi f)^2 m_1$$
$$c_1 = m_1 \pi f 0.04$$

where $f = 1\,\text{Hz}$ is the natural frequency associated with the mass of the building.

The maximum wind force, on the other hand, was approximated by

$$F_{max} = \frac{1}{2}\rho v^2 A$$

with

- $\rho \approx 1.2\,\text{kg/m}^3$, the air density;
- $v = 15\,\text{m/s}$, the wind speed;
- $A = 200 \times 30 = 6000\,\text{m}^2$, the area of one side of the building.

Scenarios considered For the uncontrollable input (wind), multiple scenarios were considered :

$$F_1 = F_{max} \quad \forall t \qquad \text{Constant wind force}$$
$$F_1(t) = F_{max}\sin(2\pi t) \qquad \text{Sinusoidal wind force}$$
$$F_1(t) = F_{max}\texttt{rand()} \qquad \text{Random wind force}$$

[2]We would like to thank Professor Denoël for discussing these values with us.

A constant force over time is not very realistic for wind but allows us to observe the behaviour of our system in the face of a very simple entry.

A sinusoidal force is also not very realistic but could correspond to multiple wind gusts on either side of the building.

A random wind is a rather realistic scenario that can model multiple wind gusts of varying intensity on either side of the building.

2.4 Stability and eigenvalues

To study the stability of the system, we computed the eigenvalues of the dynamic matrix A thanks to Matlab function (`eig`) :

$$\begin{aligned}\lambda_1 &= -0.0634 + 6.2837\text{i} \\ \lambda_2 &= -0.0634 - 6.2837\text{i} \\ \lambda_3 &= -0.1666 + 1.8179\text{i} \\ \lambda_4 &= -0.1666 - 1.8179\text{i}\end{aligned}$$

The system is stable if the real parts of the eigenvalue are all negative. In this case, the system is thus stable.

We notice that λ_1 and λ_2, being closer to the imaginary axis than λ_3 and λ_4, are two dominant eigenvalues. They therefore govern the dynamics of the system.

We also note that λ_3 and λ_4 are also very close to the imaginary axis. So our system is very responsive.

2.5 Open loop system simulations

We simulated during 30 seconds, in open loop, the different scenarios presented in section 2.3.3. We also varied the initial conditions. Since we have not yet implemented a control mechanism, the controllable input of the system is at 0 for all simulations. It can be noted that the open-loop system is already "controlled" by a tuned mass damper.

2.5.1 Initial conditions

For this simulation, we changed the initial conditions of our system without applying wind force. We have defined that the initial displacement of our building (state x_1) is $0.003\,\text{m}$.

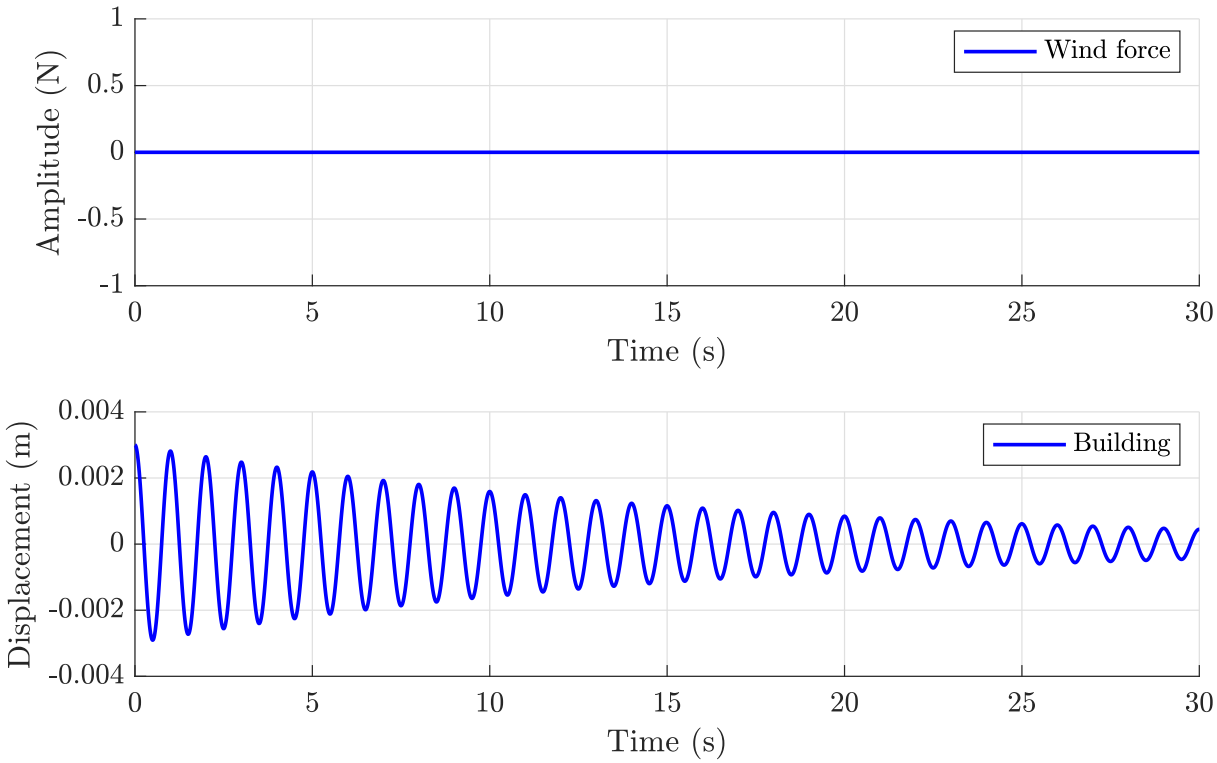

Figure 3 – Open loop simulation during 30 s with initial conditions ($x_1 = 0.003\,\mathrm{m}$)

We can see that our system is very reactive: the building oscillates quite quickly. It also quickly regains a position oscillating close to its reference position.

2.5.2 Constant wind force

For this simulation, we applied a constant wind with zero initial conditions.

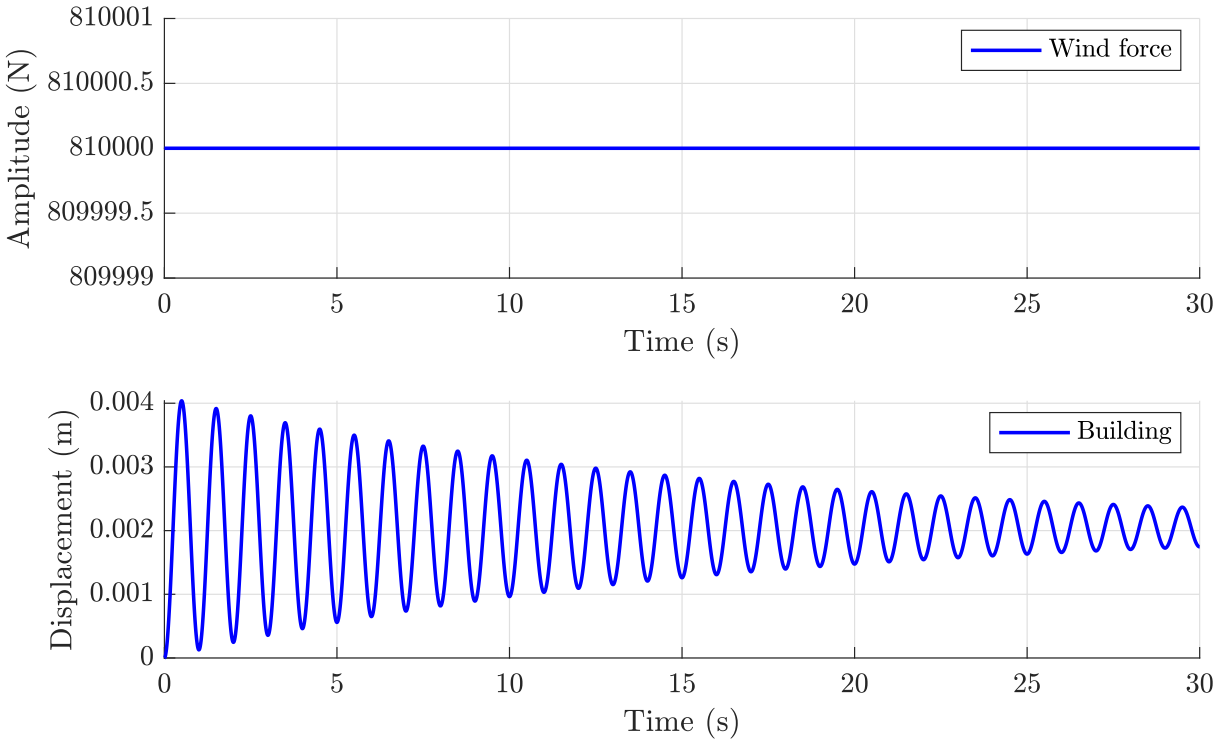

Figure 4 – Open loop simulation during 30 s for a constant wind force ($x_1 = 0\,\mathrm{m}$)

In this case, we can see that the building also oscillates very quickly. The displacement decreases quickly over time to finally oscillate around a position slightly different from its reference position.

2.5.3 Sinusoidal wind force

For this simulation, we applied a sinusoidal wind with zero initial conditions.

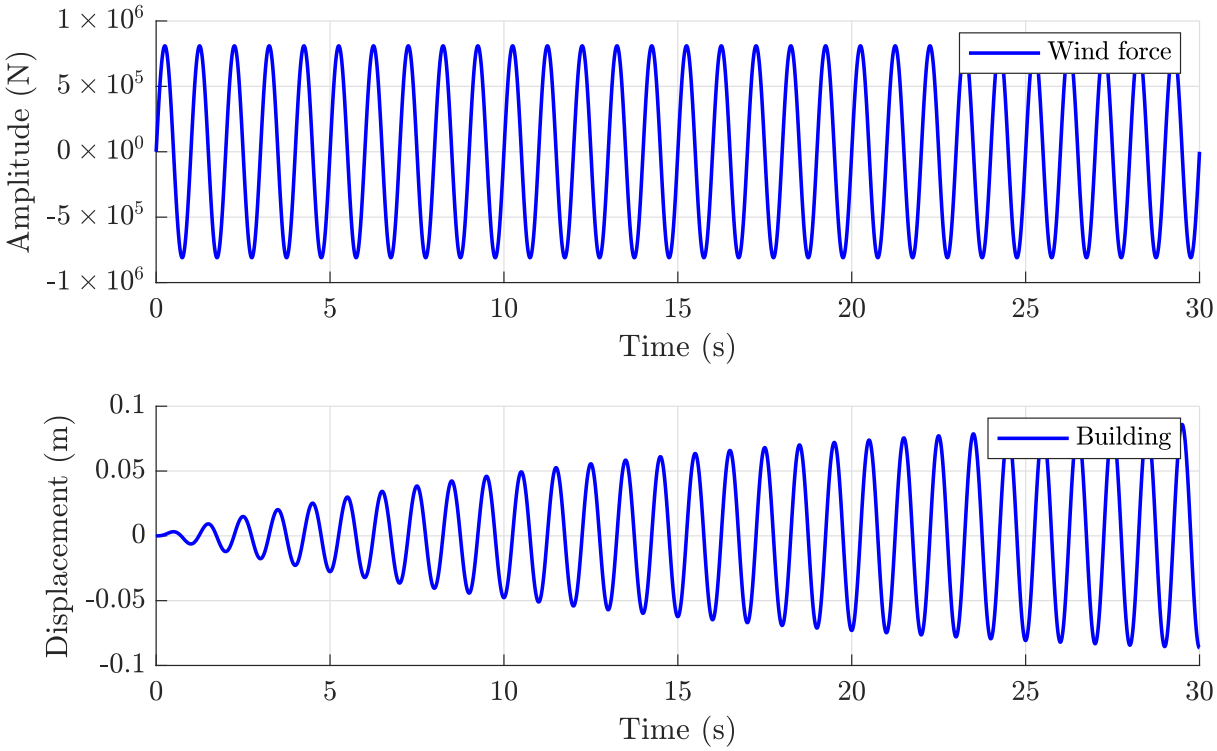

Figure 5 – Open loop simulation during 30 s for a sinusoidal wind force ($x_1 = 0\,\text{m}$)

We can see that the building's oscillations gradually increase, but quite rapidly, over time. A longer simulation has shown that these oscillations stabilize at a maximum value of 0.1 m after about 30 seconds.

2.5.4 Random wind force

For this simulation, we applied a random wind with zero initial conditions.

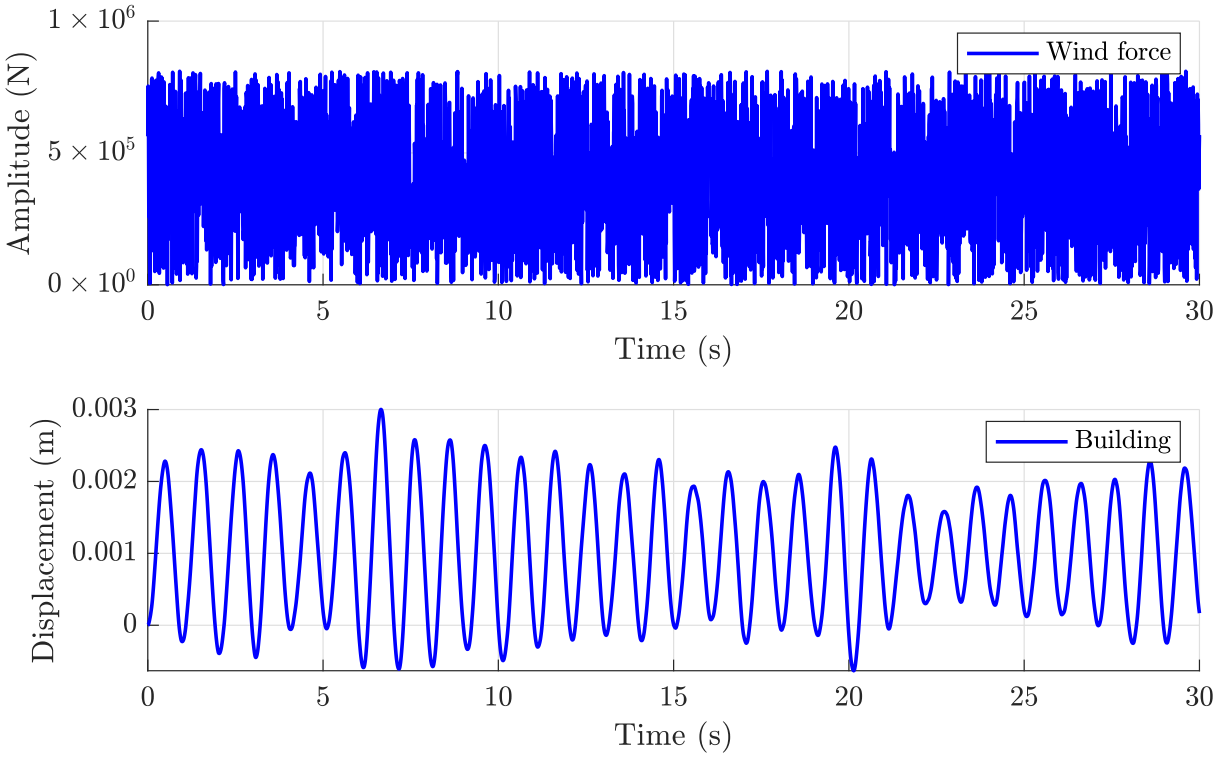

Figure 6 – Open loop simulation during 30 s for a random wind force ($x_1 = 0\,\text{m}$)

It can be seen that the building oscillates more or less identically and rapidly over time around a position slightly offset from its reference position.

2.5.5 Relation with the eigenvalues and utility of a controller

As mentioned in section 2.4, the eigenvalues of our system suggest that it is very reactive. Indeed, this has been observed on the different simulations : the building oscillates very quickly.

Eigenvalues also indicate that the system is stable. Again, this information could be found on the simulations : for a variation in initial conditions, or when the wind force is constant (or decreasing), the system tends to return to its reference position.

Although the movements of our building are quite small, a controller could reduce them even more, or even eliminate them completely after a while. Another role of the controller could be to slow down our system so that the building oscillates less quickly.

2.6 Observability

To determine whether or not the system is observable, we computed the observability matrix thanks to Matlab function (`obsv`).

The matrix is full rank (verified with Matlab), the system is thus fully observable.

As seen on the matrix C, we need one sensor. According to the place of the non zero value, this sensor has to measure the x_1 state, namely the horizontal position of the top

of the building d_1. This state is indeed the objective of the active mass damper and has thus to be observed. The sensor chosen is a position sensor (although it does not exist in that form in reality).

2.7 Controllability

To determine whether or not the system is controllable, we computed the controllable matrix thanks to Matlab function (`ctrb`). In order not to take into account the uncontrollable input (wind), only the second column of the B matrix was kept for the calculation.

The matrix is full rank (verified with Matlab), the system is thus fully controllable.

As seen on matrix B, we need only one actuator. The first column of the B matrix represents the wind, while the second one concerns the damper. This latter is indeed the only controllable input and contains two non-zero elements. As a result, only one actuator is needed, and acts on two states, the speed of the building and the speed of the damper, as they take place on x_2 and x_4. The chosen actuator is a piston.

3 Controller in time domain

3.1 State feedback controller

In a first time, we need to compute the gain matrix K.

In order not to apply a gain on the wind force, the matrix K is as follows :

$$K = \begin{pmatrix} 0 & 0 & 0 & 0 \\ g_1 & g_2 & g_3 & g_4 \end{pmatrix}$$

Indeed, the first column of matrix B concerns the uncontrollable input, so matrix K cannot affect these values.

The new dynamic matrix of the closed-loop system is $A_{CL} = A - BK$. Let's determine the eigenvalues of that matrix.

As we have a matrix of dimension 4, the approximation of the dominant poles will be done. Indeed, we have, from the previous matrix A, the eigenvalues :

$$\begin{aligned} \lambda_1 &= -0.0634 + 6.2837\text{i} \\ \lambda_2 &= -0.0634 - 6.2837\text{i} \\ \lambda_3 &= -0.1666 + 1.8179\text{i} \\ \lambda_4 &= -0.1666 - 1.8179\text{i} \end{aligned}$$

As already discussed in section 2.4, one can see that λ_3 and λ_4 are about 10 times bigger than the last two. They are not dominant when affecting the dynamics of the system, and will therefore remain in A_{CL}, although slightly modified, as explained after.

Imposing that $(s - \lambda_3)(s - \lambda_4)$ is part of the decomposition, we get that the determinant of A_{CL} is equal to :

$$(s - \lambda_3)(s - \lambda_4)(s^2 + 2\zeta\omega_c s + \omega_c^2) = 0$$

Since λ_3 and λ_4 are fixed, we only need to solve the equation of the second degree in s in order to find the expressions of λ'_1 and λ'_2 as a function of ζ and ω_c.

The solutions of the equation are given by :

$$\begin{cases} \lambda'_1 = -\zeta\omega_c - \omega_c\sqrt{\zeta^2 - 1} \\ \lambda'_2 = -\zeta\omega_c + \omega_c\sqrt{\zeta^2 - 1} \end{cases}$$

The values of ζ and ω_c will be determined by simulations in the following sections. When these have been fixed, the values of the 4 poles of A_{CL} will be obtained. Then we will just have to use the `place` function of Matlab to obtain the values g_i of matrix K associated with the eigenvalues.

However, as previously noted via simulations, our system is very reactive. The two non-dominant eigenvalues thus have also been modified in order to slow down the system. We finally obtain the expressions of the 4 eigenvalues of the controller :

$$\begin{cases} \lambda'_1 = -\zeta\omega_c - \omega_c\sqrt{\zeta^2 - 1} \\ \lambda'_2 = -\zeta\omega_c + \omega_c\sqrt{\zeta^2 - 1} \\ \lambda'_3 = \mathbb{R}(\lambda_3)0.5 + \mathbb{I}(\lambda_3)i \\ \lambda'_4 = \mathbb{R}(\lambda_4)0.5 + \mathbb{I}(\lambda_4)i \end{cases}$$

As the reference is 0, k_r has not to be considered, so it can fixed to 0.

However, some tests of a change in reference will be performed in this report. We therefore calculated k_r using the following formula :

$$k_r = \frac{-1}{C(A - BK)^{-1}B}$$

where only the controllable part of matrix B (second column) and the non-zero row of K were considered. Indeed, if the entire matrices were used, it would mean that we would have an action on the uncontrollable input, which is not possible.

3.2 Observer

The controllable input being a linear combination of the different states multiplied by gains, the control system requires the different states as inputs. However, the open loop system only provides one output.

Considering that the real states cannot be measured in practice, the observer is a tool that allows us, based only on the output of the open loop system and on the inputs, to approximate the different states of the system.

Its realization must be such that the convergence of the estimated states with the real states is as fast and correct as possible.

One thus needs to compute the gain matrix L :

$$L = \begin{pmatrix} l_1 \\ l_2 \\ l_3 \\ l_4 \end{pmatrix}$$

The new dynamic matrix is given by $A_{obs} = A - LC$.

As previously, we will keep the same two non-dominant eigenvalues and determine the two other via the same method that has been used for K.

Imposing that $(s - \lambda'_3)(s - \lambda'_4)$ is part of the decomposition, we get that the determinant of A_{obs} is equal to :

$$(s - \lambda'_3)(s - \lambda'_4)(s^2 + 2\zeta\omega_c s + \omega_c^2) = 0$$

Since λ'_3 and λ'_4 are fixed, we only need to solve the equation of the second degree in s in order to find the expressions of λ_1^* and λ_2^* as a function of ζ and ω_c.

The solutions of the equation are given by :

$$\begin{cases} \lambda_1^* = -\zeta\omega_c - \omega_c\sqrt{\zeta^2 - 1} \\ \lambda_2^* = -\zeta\omega_c + \omega_c\sqrt{\zeta^2 - 1} \end{cases}$$

The poles of the observer are determined by taking the poles of the controller and moving them. To do this, the real parts of each pole are multiplied by a constant α. In the case of poles λ'_1 and λ'_2, this amounts to multiplying ω_c by α.

We finally have :

$$\begin{cases} \lambda_1^* = -\zeta\omega_c\alpha - \omega_c\alpha\sqrt{\zeta^2 - 1} \\ \lambda_2^* = -\zeta\omega_c\alpha + \omega_c\alpha\sqrt{\zeta^2 - 1} \\ \lambda_3^* = \mathbb{R}(\lambda'_3)\alpha + \mathbb{I}(\lambda'_3)i \\ \lambda_4^* = \mathbb{R}(\lambda'_4)\alpha + \mathbb{I}(\lambda'_4)i \end{cases}$$

The values l_i of the matrix L are then obtained by using the `place` function of Matlab. The chosen values are given in the next section.

3.3 Simulations and discussion

3.3.1 Parameter determination

In order to best achieve our control system, we must determine the values of ζ, and ω_c. We know that the system control is done via the controllable input $u(t)$, and that this input will influence the variation of the output and the different states of the system.

In order to obtain a coherent system, *i.e.* physically possible state values and an attenuation of building oscillations, we must choose values of ζ and ω_c that will lead to a control input making the system coherent.

We tested several values of ζ as well as several values of ω_c with a constant wind force :

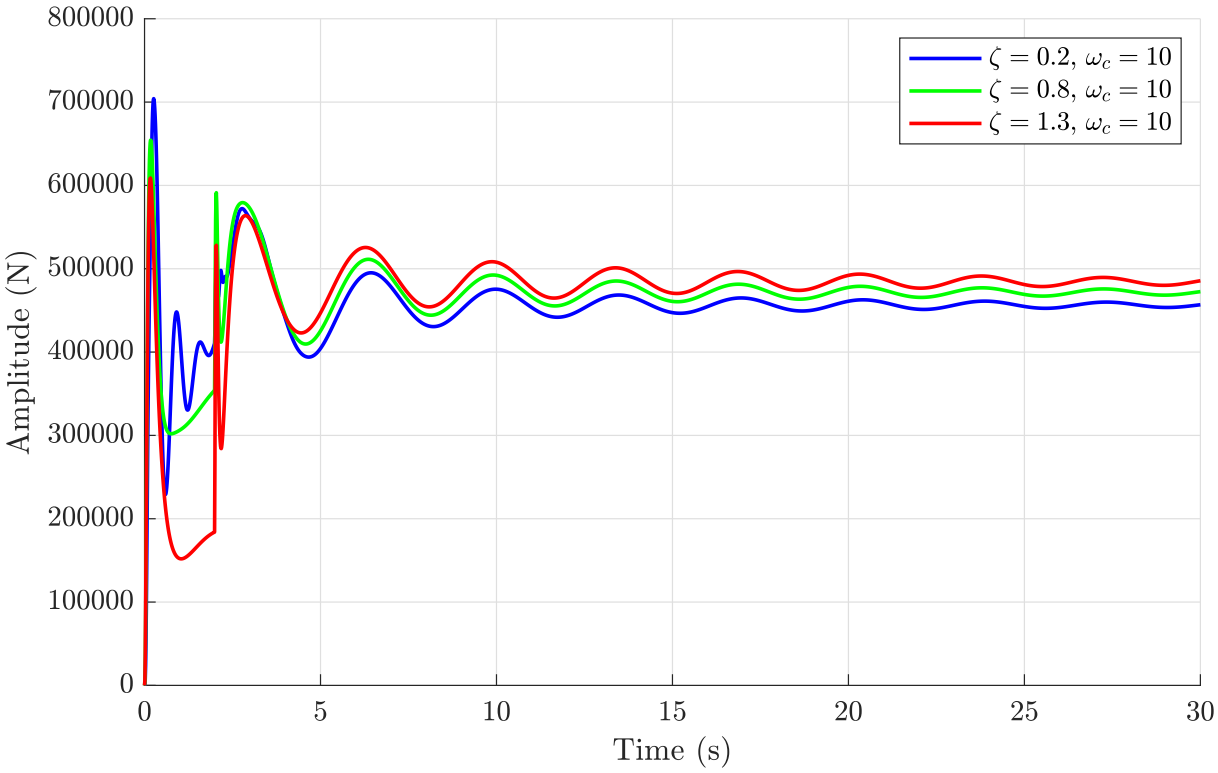

Figure 7 – Control input $u(t)$ for different variations of parameter ζ

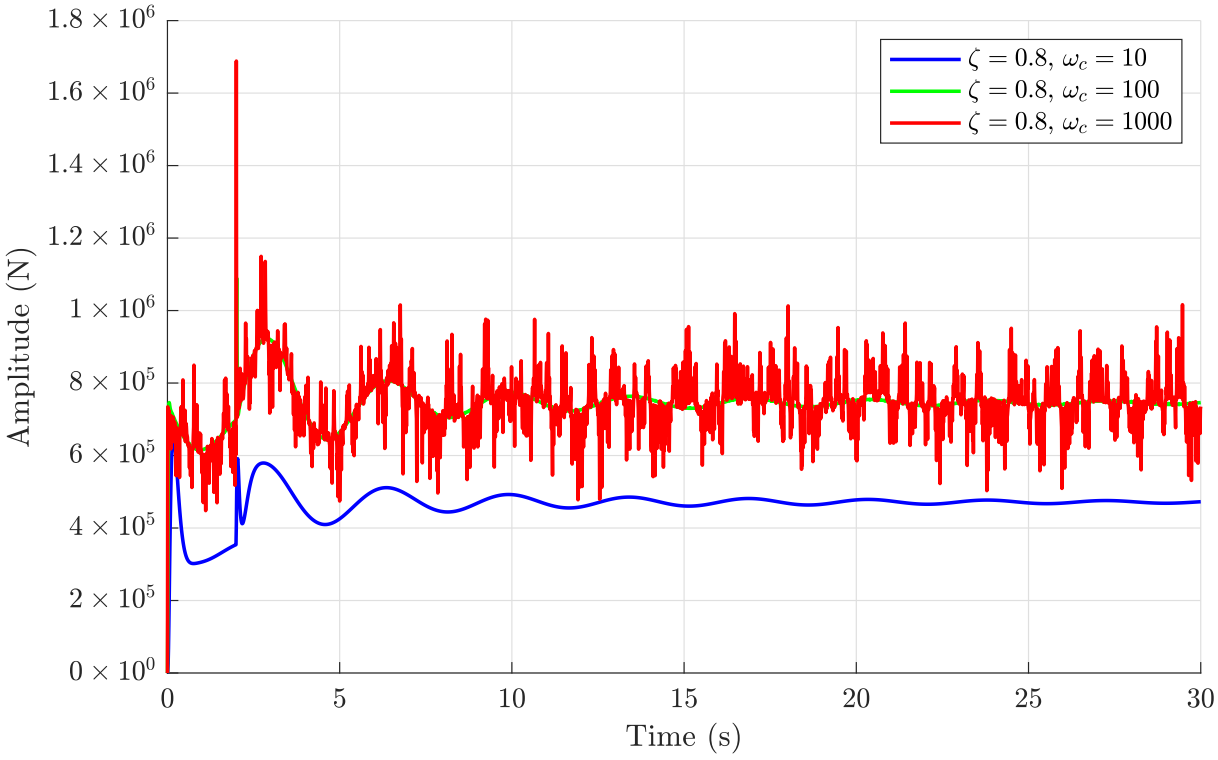

Figure 8 – Control input $u(t)$ for different variations of parameter ω_c

It can be seen that the variations in parameter ζ have little influence on the controllable force : after a few seconds, it is identical in all cases.

Concerning the parameter ω_c, we observe that the higher it is, the faster the control force oscillates (which is an undesirable behaviour).

We also observed the variation of the parameter ω_c on the states x_1 (also the output) and x_3 of our system :

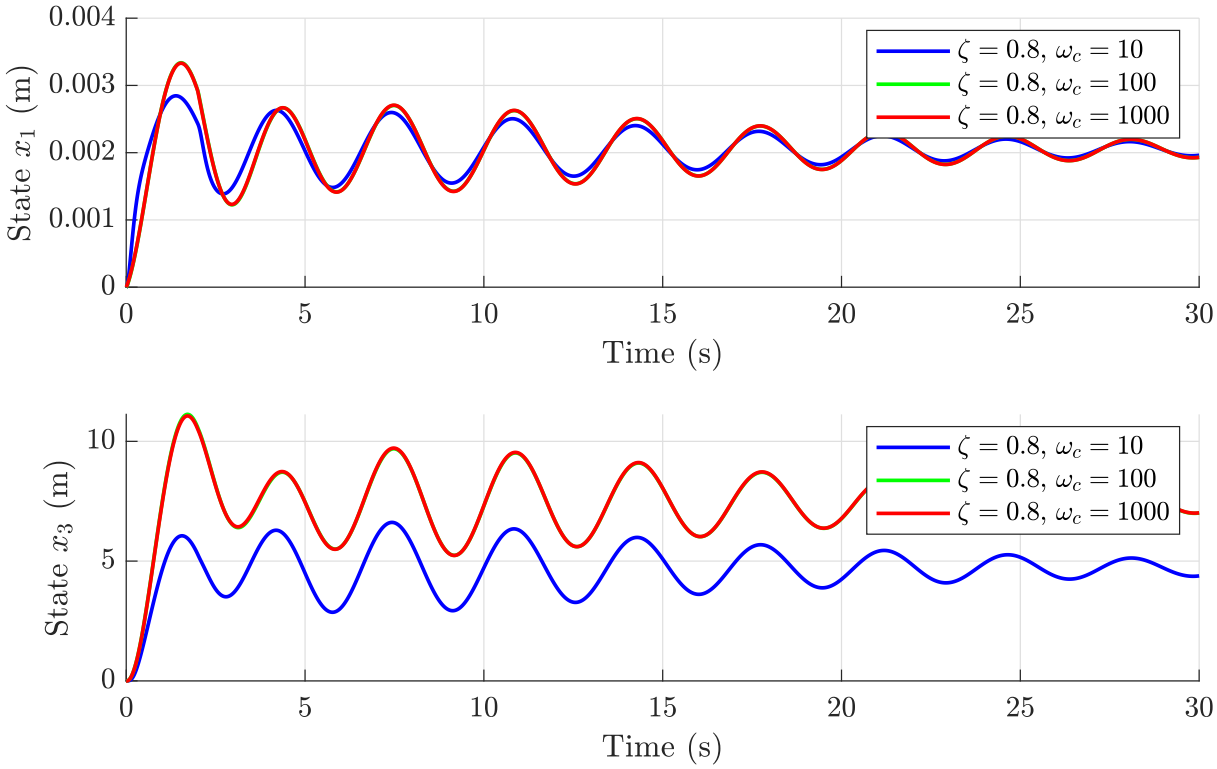

Figure 9 – States x_1 and x_3 of the system for different variations of parameter ω_c

First of all, we observe that the green and red curves overlap perfectly. Then, we find that the influence of the ω_c parameter on the states is relatively small. Only the damper's behaviour varies considerably.

The variations of the x_2 and x_4 statements are very similar and lead to the same observations.

The parameter ζ has little influence on the controllable input, so the variations of the states according to its different values are also small and we have chosen not to highlight them in this report.

We also checked the influence of these parameters on a variation of the reference and on a noisy input. The observations are identical to those made on the statements (slight variations for ω_c and some slight variations for ζ).

We therefore choose to take the following values of the parameters :

$$\begin{cases} \zeta = 0.8 \\ \omega_c = 10 \end{cases}$$

We also arbitrarily choose our parameter $\alpha = 5$. This choice, in regards of the simulations presented later, is proving to be a good one.

These values allowed us to calculate the eigenvalues of the matrices A_{CL} and A_{obs} and thus to obtain our matrices K and L :

$$\begin{cases} \lambda'_1 = -8.0000 + 6.0000\text{i} \\ \lambda'_2 = -8.0000 - 6.0000\text{i} \\ \lambda'_3 = -0.0833 + 1.8179\text{i} \\ \lambda'_4 = -0.0833 - 1.8179\text{i} \end{cases} \qquad \begin{cases} \lambda^*_1 = -3.3057 \\ \lambda^*_2 = 0.0734 \\ \lambda^*_3 = 0.0064 + 0.0259\text{i} \\ \lambda^*_4 = 0.0064 - 0.0259\text{i} \end{cases}$$

With these different values, our control input is as follows :

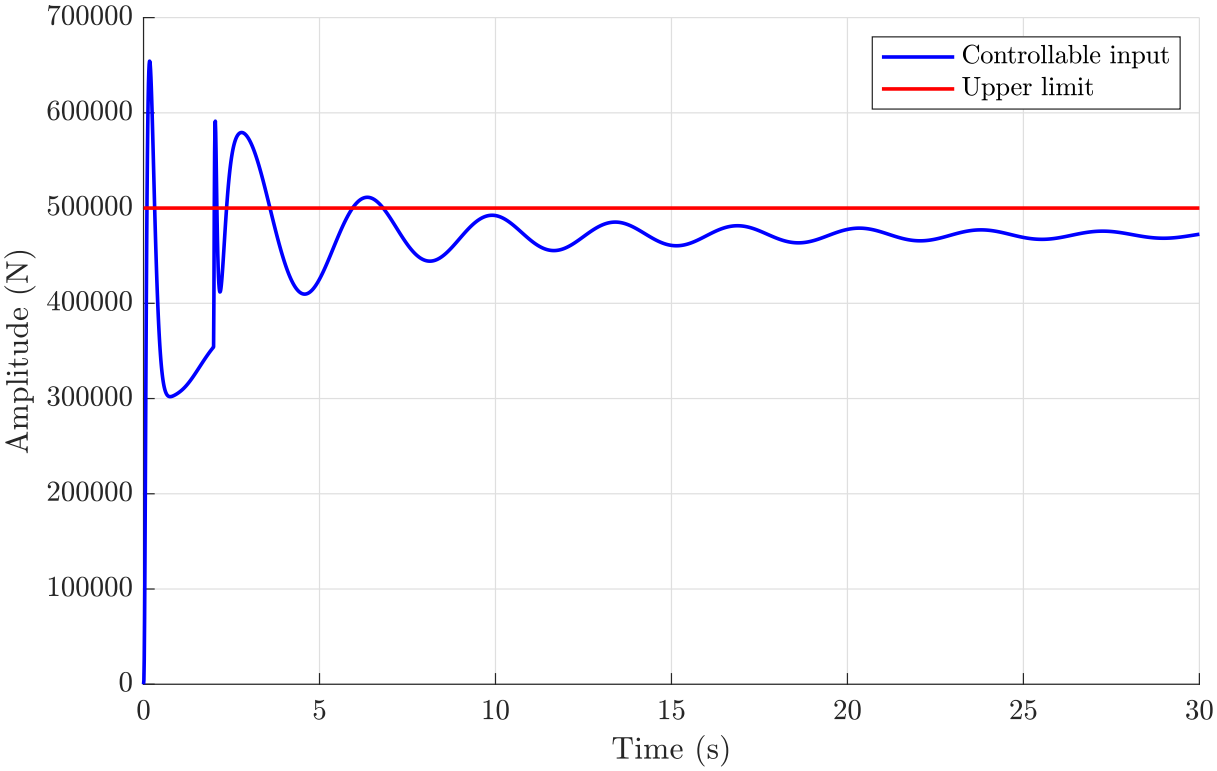

Figure 10 – Control input $u(t)$ for $\zeta = 0.8$ and $\omega_c = 10$

An abnormally high peak is observed at the beginning. This peak is due to the unrealistic simulations performed : the simulation goes from a zero wind to a constant wind of several thousand newtons in an instant (similar to a step). However, it can be seen that after this peak, the control force oscillates around much more realistic values within our previously defined acceptable range of values.

This control input does allow a reduction in building oscillations, and this in a relatively slower way (the system has been slowed down).

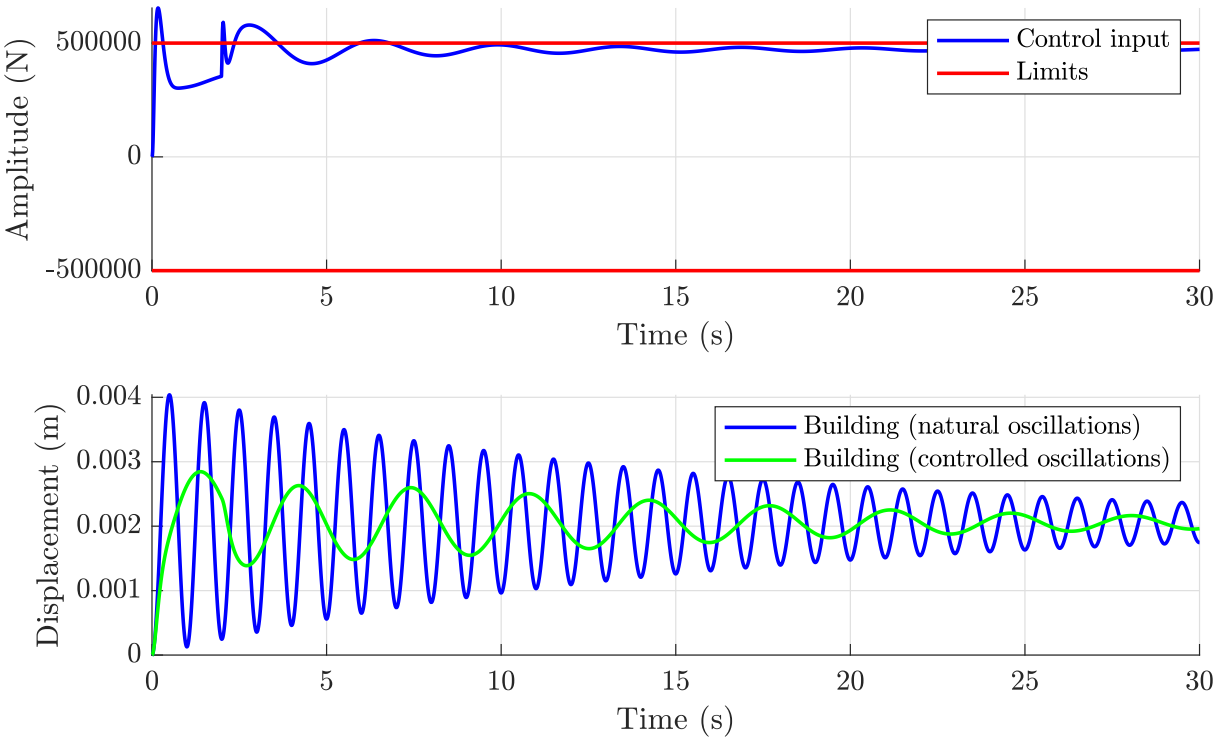

Figure 11 – System simulation with and without control input for a constant wind.

We can now evaluate the performance of our observer. To do this, we launched a 10-second simulation with a sinusoidal wind force. In order to observe its convergence, the controlled system and observer have different initial conditions and a time delay upon entry (2 s).

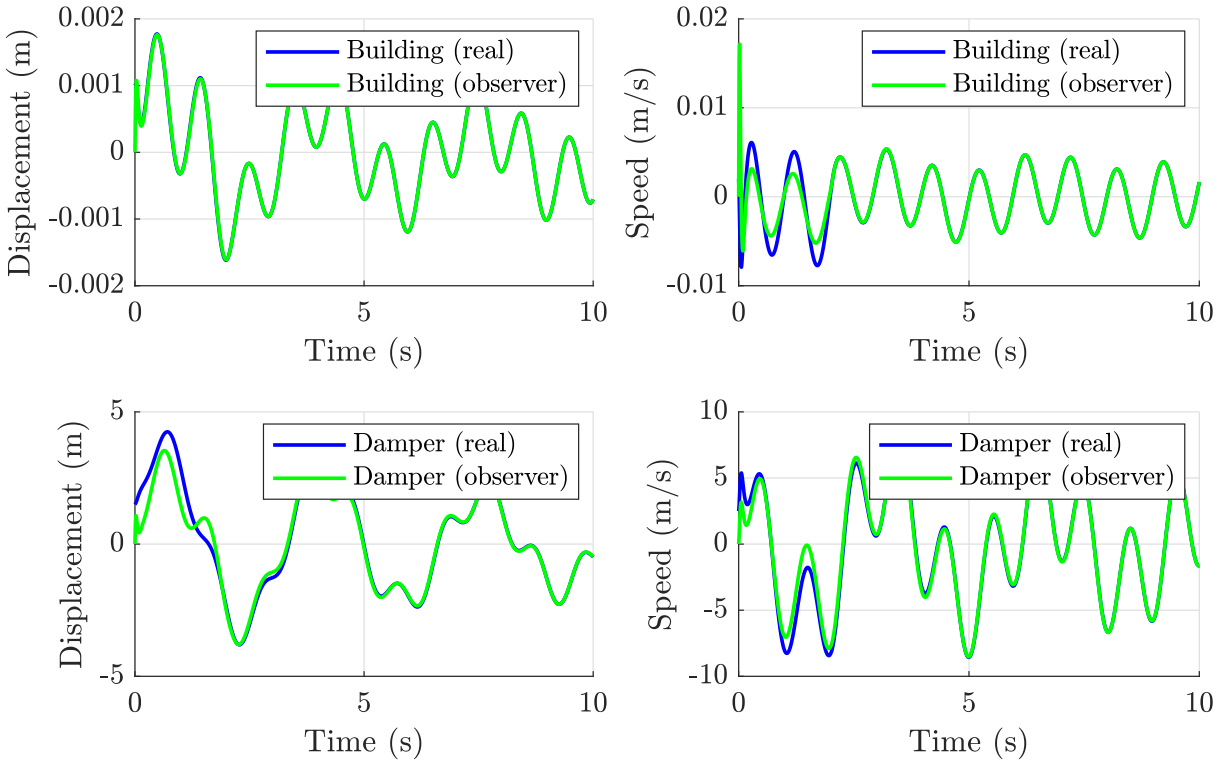

Figure 12 – Simulation of the observer with a sinusoidal wind force

We notice that our observer converges very quickly (5 seconds maximum, 10 for absolute convergence) towards the real states of the system. Its realization seems to be correct.

We can also see that the values of our states, with the control system in place, seem to be consistent and within the plausible value domains we defined earlier.

We will now study the behaviour of the system in several situations. We have not plotted the influence of ζ and ω as they have an almost identical behaviour as for the previous discussions that led to their determination.

3.3.2 Response to a reference variation

For this simulation, we have set the uncontrollable input to 0 and changed the reference to 0.002 m.

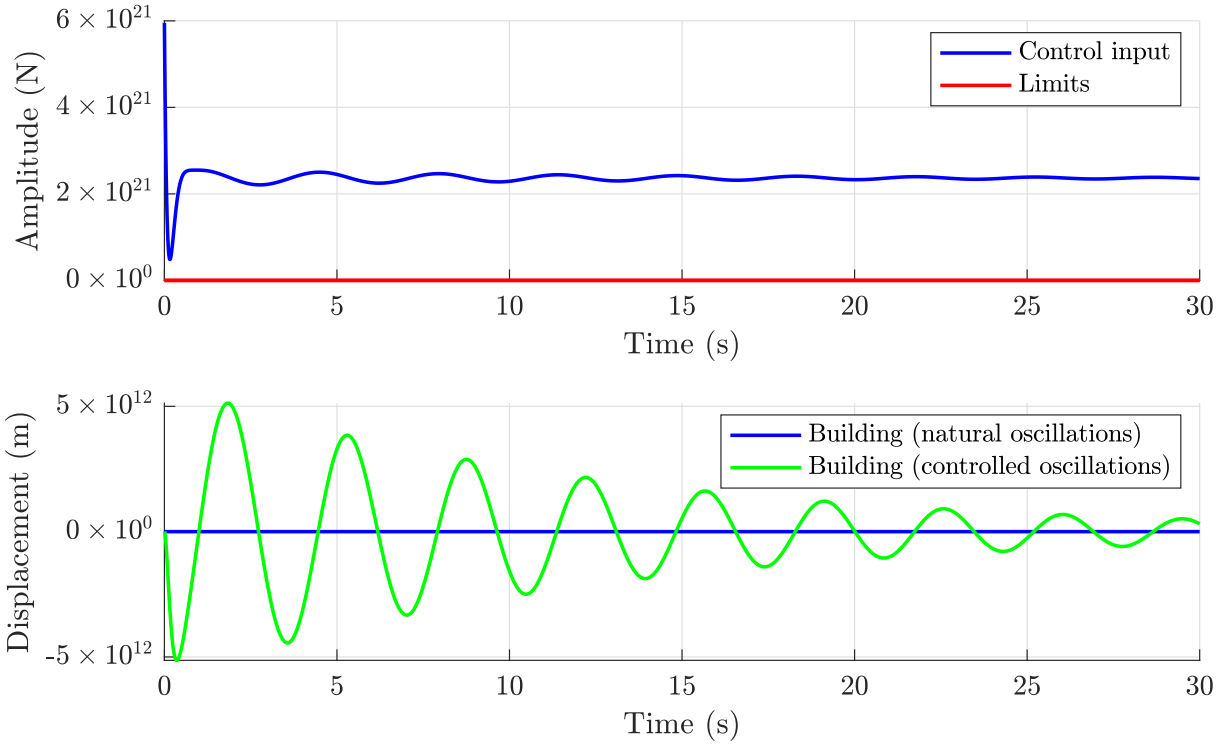

Figure 13 – System simulation with a reference variation of 0.002 m

We observe that the values of the controlled signal are totally incoherent. We have not found where this problem comes from. We have designed k_r so that the system is robust to reference variations. The expected behaviour is therefore not normal nor intended.

However, the reference of our building is not supposed to change over time, and being resistant to that kind of change is not something we think is needed for this instance.

3.3.3 Response to a perturbation (disturbance)

We simulated our different wind scenarios to see how the controlled system reacts. The constant wind scenario has already been presented in figure 11. We therefore simulated the two remaining scenarios.

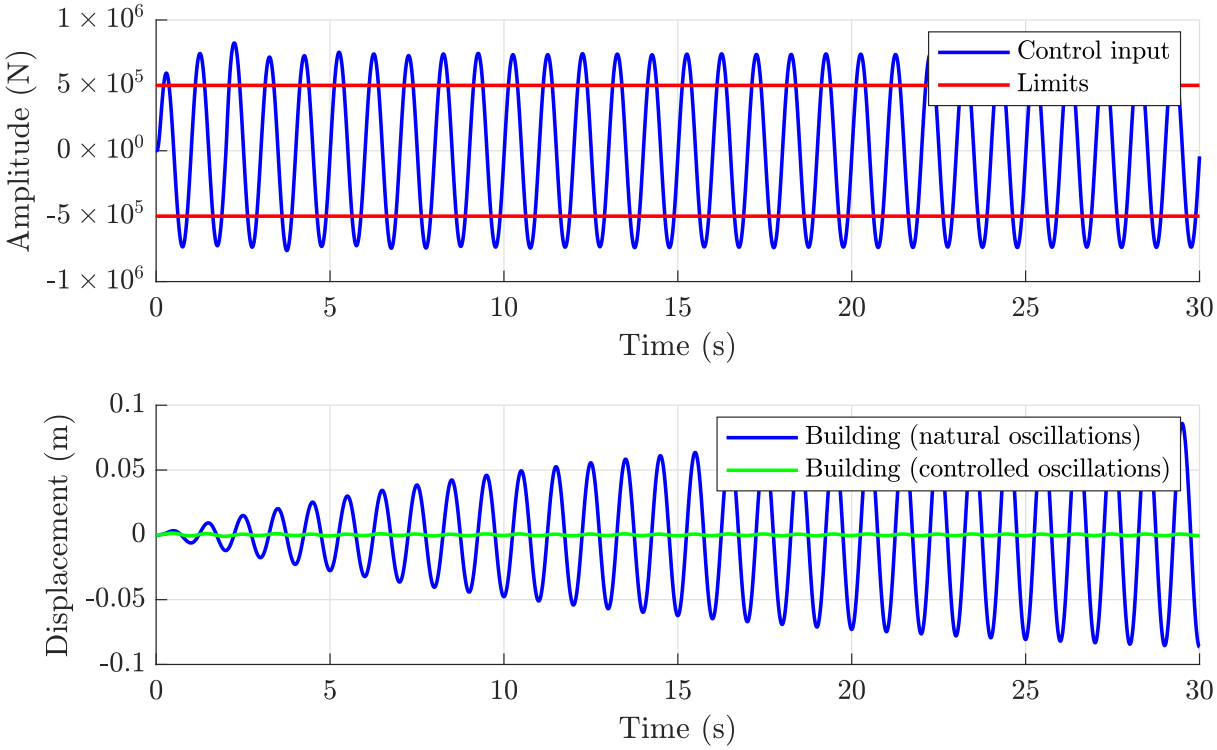

Figure 14 – System simulation with a sinusoidal wind force

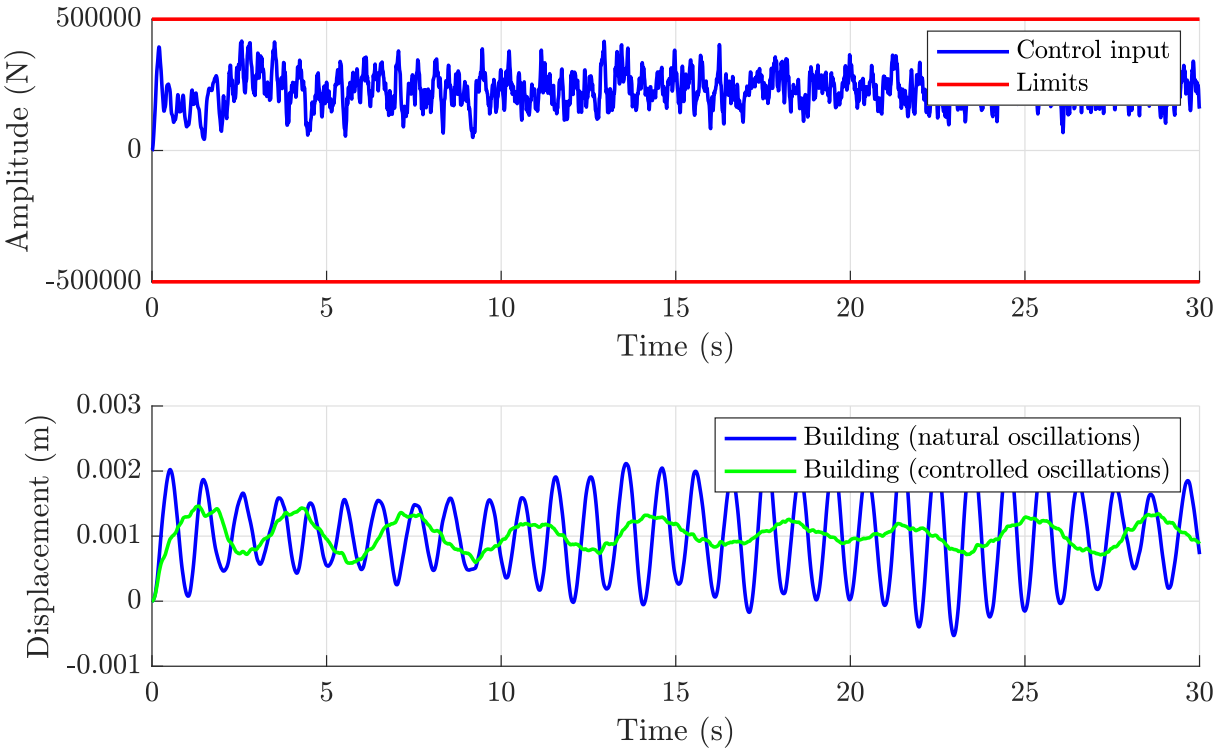

Figure 15 – System simulation with a random wind force

For each of the scenarios, we can see that the oscillations of the buildings are attenuated

and tend to disappear completely quite quickly. The controlled system is much slower than the initial system.

Our control therefore seems to be fulfilling its role well, although the force we need to apply to our controller is sometimes a bit too high compared to our constraints. We have spent hours trying to reach these constraints by tweaking the parameters of our controller, but this is the best we could manage. More information on that is given in the general conclusion.

3.3.4 Presence of noise

For this simulation, we added a random noise (approximately 5% of the nominal value) to the inputs of the observer (so the output of the controller and the delayed disturbance of the observer). This noise will influence the control input, and therefore the system output.

The control input affected by noise is shown in figure 16.

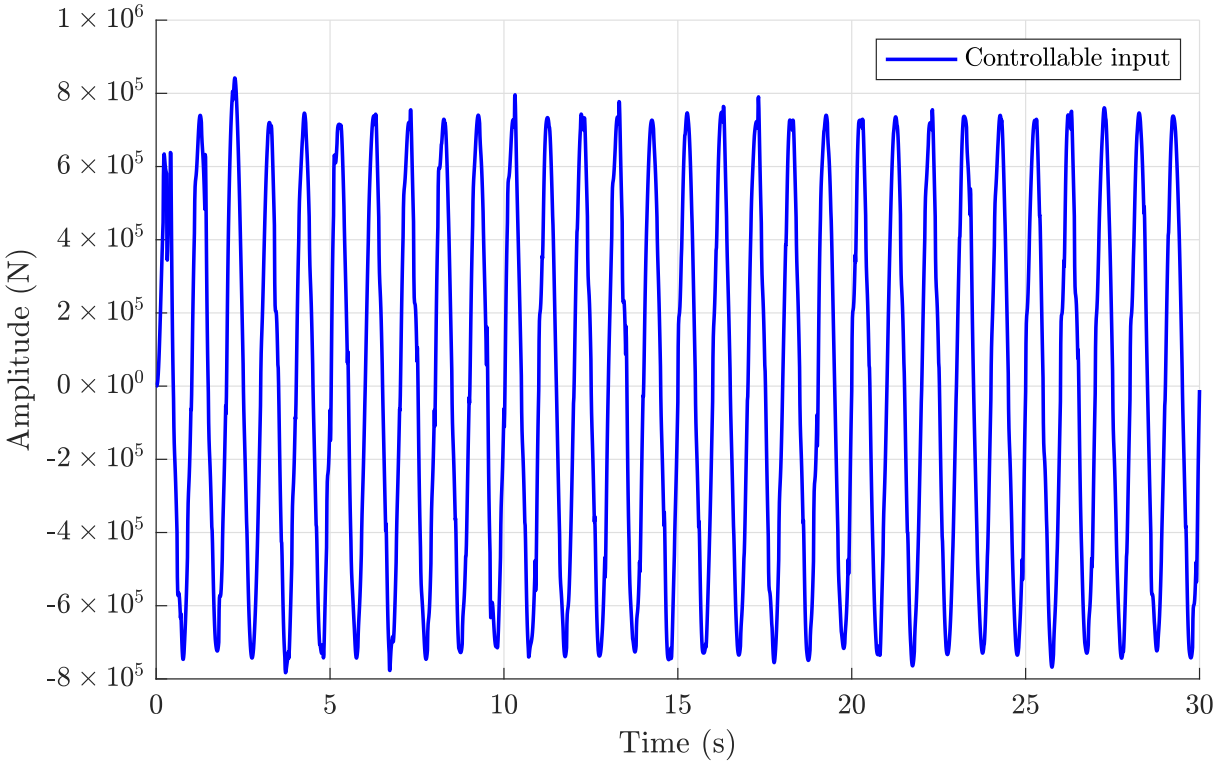

Figure 16 – Control input $u(t)$ with noise in the observer

The system output (as well as the original disturbance) is shown in figure 17.

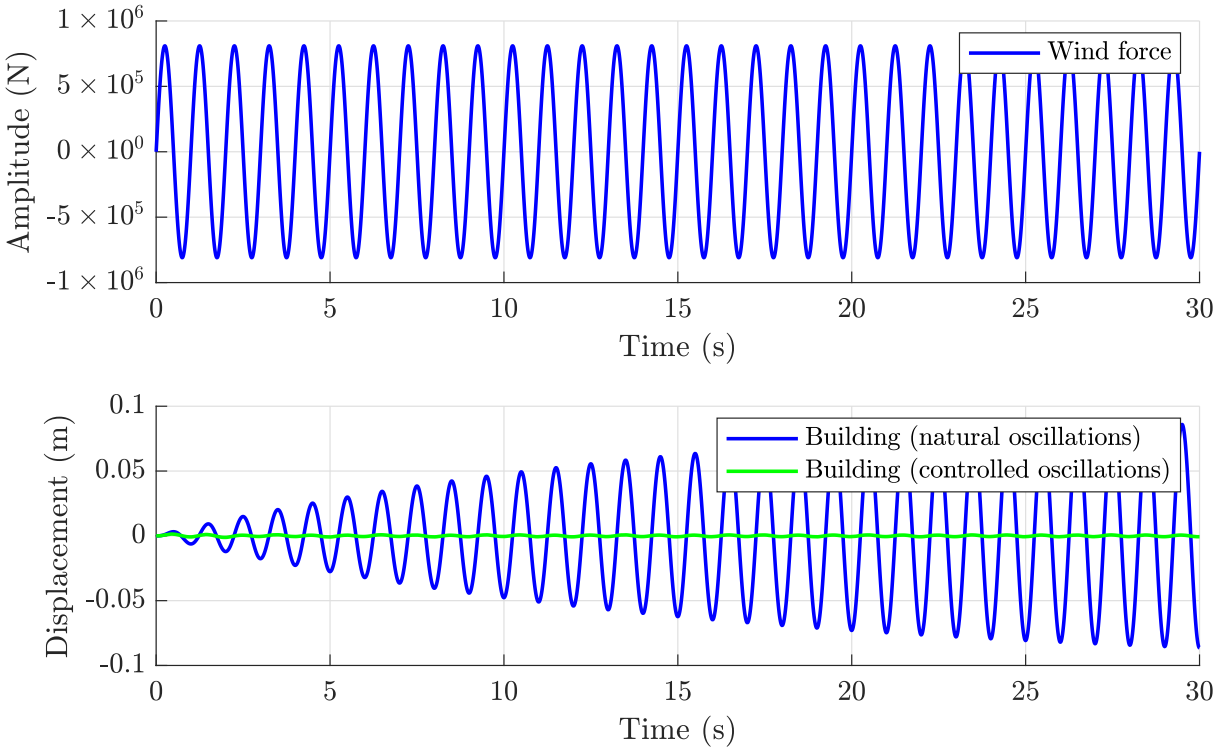

Figure 17 – System simulation with noise in the observer

We see that our system is robust to noise. Indeed, despite the presence of the latter, the building's oscillations are still very well attenuated. A try for an explanation is given in the general comparison between the two controllers.

4 Controller in frequency domain

4.1 Framework

For this part of the work, it has decided to simplify our system and use 2 states instead of 4. The position and speed of the damper are therefore hidden in the force of the actuator, which is still the controllable input of the system.

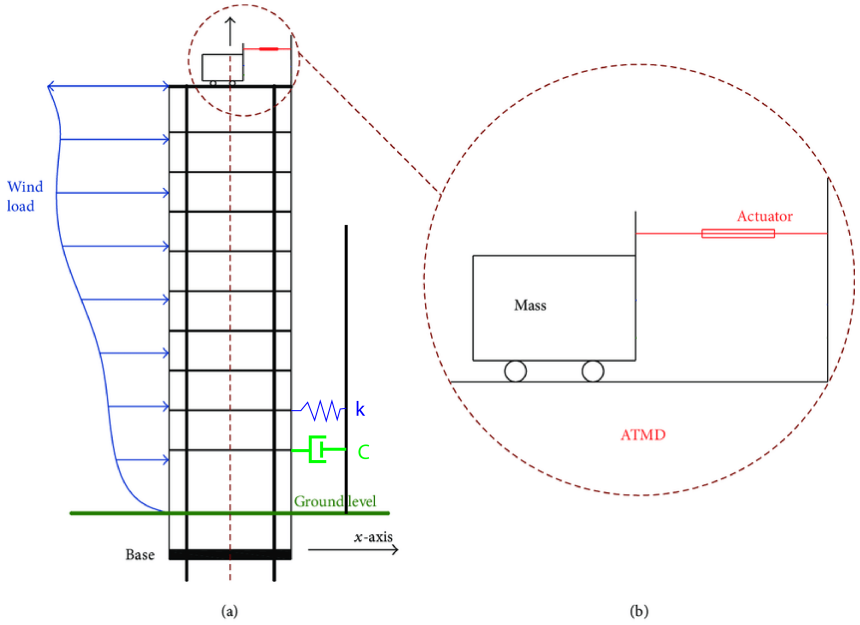

Figure 18 – Simplified system of an active mass damper

The law that governs that system is the following :

$$m_{tot}\ddot{x} + c\dot{x} + kx = F_{wind} + F_{damper}$$

where

- $F_{damper} = m_{damper}a_{damper}$
- $m_{tot} = m_{building} + m_{damper}$
- x is the position of the building relative to its rest position ($x = 0$)

Let's now define the input, output and states :

- $u_1 = F_{wind}$
- $u_2 = F_{damper}$
- $x_1 = x$
- $x_2 = \dot{x}$
- $y = x_1$

By doing so, the ABCD matrices are the following :

$$A = \begin{pmatrix} 0 & 1 \\ \dfrac{-k}{m_{tot}} & \dfrac{-c}{m_{tot}} \end{pmatrix} \quad B = \begin{pmatrix} 0 & 0 \\ \dfrac{1}{m_{tot}} & \dfrac{1}{m_{tot}} \end{pmatrix}$$

$$C = \begin{pmatrix} 1 & 0 \end{pmatrix} \quad D = \begin{pmatrix} 0 & 0 \end{pmatrix}$$

4.1.1 Constraints and simulation specifications

We have the following constraints :

- Acceleration of the mass damper below $1.6g$, to be consistent with the time domain.
- Lateral movement of the top of the building not above 1 m.

The two scenarios we look at are the following : a turbulent wind of maximum 810 kN, that is represented as a sine function and a constant wind of the same intensity (the random wind has been studied and is referenced but is not plotted for this section).

Here are the values of the different parameters that have been chosen, as previously :

Mass	$m_{building} = 1 \times 10^7\,\mathrm{kg}$	$m_{damper} = 3 \times 10^4\,\mathrm{kg}$
Spring	$k \approx 4 \times 10^8\,\mathrm{N\,m^{-1}}$	
Damper	$c \approx 1.3 \times 10^6\,\mathrm{N\,s\,m^{-1}}$	
Wind	$F_{max} = 810\,\mathrm{kN}$	

Table 4 – Numerical values of the system

4.1.2 Choice of cross-over frequency

The frequency of the building is of about 1 Hz, as advised by Pr. Denoël, and the frequency of the sinusoidal wind studied is also of 1 Hz. So the cross-over frequency was initially set at 5 Hz.

All frequencies above that, probably coming from noise and unwanted phenomena, will be attenuated, while the amplitudes of the frequencies below that, which correspond to the internals of the system, will be amplified.

In the end, after some simulations, we have decided to put the crossover frequency at $20\,\mathrm{rad\,s^{-1}}$ as we have found out that a smaller crossover frequency induces a slightly slower response in our system. Although not noticeable in the sinusoidal force scenario, it can be seen when the disturbance is a constant or a random function.

4.2 Transfer function of the open-loop system

4.2.1 Computation

For the computation of the transfer function of our system, we used the Matlab function `tf(sys)` then selecting the answer corresponding to our controllable input. In our case,

$$P(s) = \frac{9.97e-8}{s^2 + 0.1257s + 39.48}$$

Had we wanted to compute it by hand, we would have translated our ABCD system to its frequency form (derivative becomes a multiplication by s), then we would have found that

$$H(s) = \frac{Y(s)}{U(s)} = C(sI - A)^{-1}B + D$$

By selecting only the columns of B and D corresponding to the controllable input, we would have found the same expression as the one above.

4.2.2 Plots

The Bode plots of the open-loop system are given at figure 19.

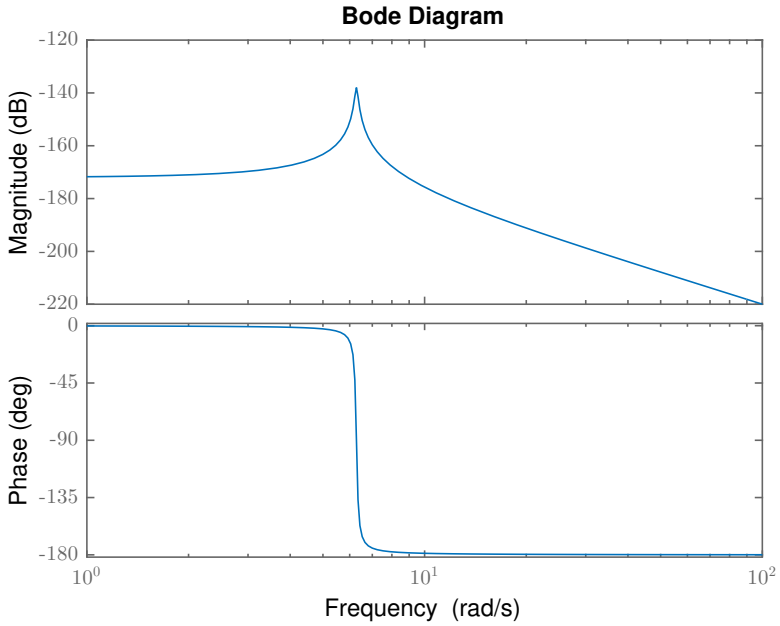

Figure 19 – Bode plots for 2D system

These graphs have the typical shape of the second order systems. If we confront our transfer function with the typical transfer function of such a system ($H(s) = \frac{1}{s^2+2\zeta\omega_n s+\omega_n^2}$), we find that $\omega_n \approx 6.28$ and $\zeta \approx 0.01$.

We thus have two complex poles, oscillations and overshoots. The peak is quite high, as $\zeta \ll 1$, and the transition from $0°$ to $-180°$ (at ω_n, the natural frequency of our system) is quite sharp for the same reasons.

4.3 Loop shaping

4.3.1 Lag compensator

Firstly, we have decided to use a lag compensator in order to increase the gain for low frequencies (remove the flat area at low frequencies) and thus have a better response. We have used a lag compensator of the following shape :

$$Glag(s) = \frac{s+a}{s}$$

The bode diagram of that transfer function is given at figure 20.

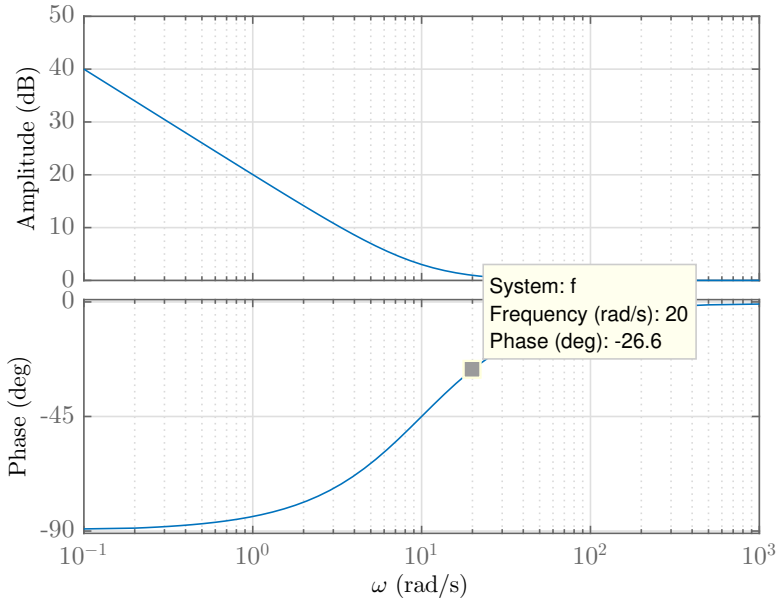

Figure 20 – Bode diagrams of the lag compensator

We have decided to use a a of 10 to attenuate the natural frequency spike in the initial Bode amplitude diagram without interfering too much with the phase diagram (a is used to move the point at which the amplitude of the Bode diagram becomes 0 dB).

As can be seen, this element induces a phase of about $-26°$ at the crossover frequency, but it is not a problem as we have succeeded in tuning our lead compensator to be resistant to the delays we will have in our system. It can be noted that, for a sinusoidal wind, the use of such a component is not necessary. However, when we conducted tests with a constant wind (equivalent to a step), we have found out that using a lag compensator induces no static error while not using one induces a stabilization at a position different from the reference.

However, the acceleration of the damper becomes twice as large as those with no lag compensator. We have decided to keep it to comply with the theoretical shape of the desired Bode diagram but, in practice, if the acceleration is too intense with such a component, we could easily remove it without bringing instabilities in the response of the building.

4.3.2 Lead compensator

Let's now add a lead compensator to obtain the desired phase margin. Delays are discussed after, but we want to be able to respond at least to 0.02 s delays, which correspond to the 50 Hz of the actuator's piston [4].

We have finally decided to use a phase margin of 80° for the following computations, although it will translate in practice to a phase margin of 42° because of interference with the lag compensator and the low-pass filter. In order to increase the phase margin at the

crossover frequency, we have decided to use a lead compensator.

Its transfer function is given by :

$$G(s) = \frac{\frac{s}{w_z} + 1}{\frac{s}{w_p} + 1}$$

For a given crossover frequency ω_{co} and a phase margin ϕ_m, we can determine the two w (further apart means a phase and amplitude modifications in L more spread) in the following way :

$$\begin{cases} w_z = \tan(\alpha) w_{\text{co}} \\ w_p = \frac{w_{\text{co}}}{\tan(\alpha)} \end{cases}$$

with $\alpha = \frac{\pi}{4} - \frac{\phi_m}{2}$.

For the crossover frequency and the desired value of ϕ_m, we have that that :

$$w_z = 1.75 \qquad w_p = 228.6$$

We have chosen that phase margin because, with one below 65°, the delays we have determined bring instability to our system, as we have seen in the Nyquist diagrams. Any value above that is fine in that regards and does not impact our output and controllable input in a very determinant way. However, lower phase margins tend to slightly increase the speed of our control system, so we have chosen this phase margin of "80°". The Bode plots of this component is given at figure 21.

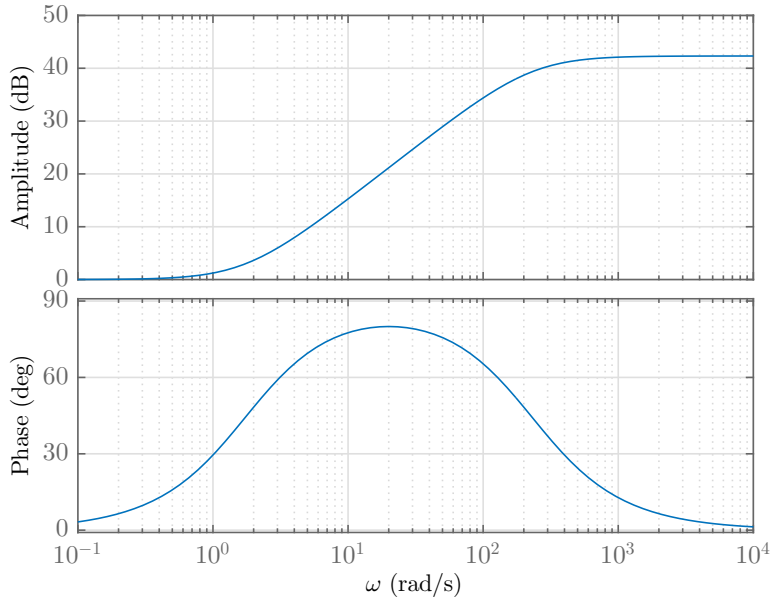

Figure 21 – Bode diagrams of the lead compensator

4.3.3 Gain

After that, one needs to add a gain to our system in order to increase the amplitude gains for all frequencies and make it so that the amplitude is at 0 dB at the crossover frequency.

That is done by using a constant gain. This does not affect the phase but increases the amplitudes of about 175.5 dB, which positions our Bode plot to where one wanted it to be.

4.3.4 Low-Pass Filter

$$G(s) = \frac{1}{\frac{s}{a} + 1}$$

We have decided to use a low-pass filter in order to attenuate even more the gains for higher frequencies.

In the case of a random wind, we have seen that it reduces a bit the spikes in the controllable input, so we have decided to keep it, although its action for other scenarios was not perceived. However, such a filter is designed to attenuate the effect of noise on the system, and in that regards, it works quite well with our system, as we can see in the section dedicated to noise at the end of this report.

As can be seen on the Bode diagrams at the figure 22, we induce a loss in phase of about 11° by choosing a parameter $a = 5 * \omega_{co}$ for the low-pass filter. However, as it has already been said for the lag compensator, the system can still react well to the delays we have identified. If it did not, we could use a bigger a, but we would react less nicely to noise.

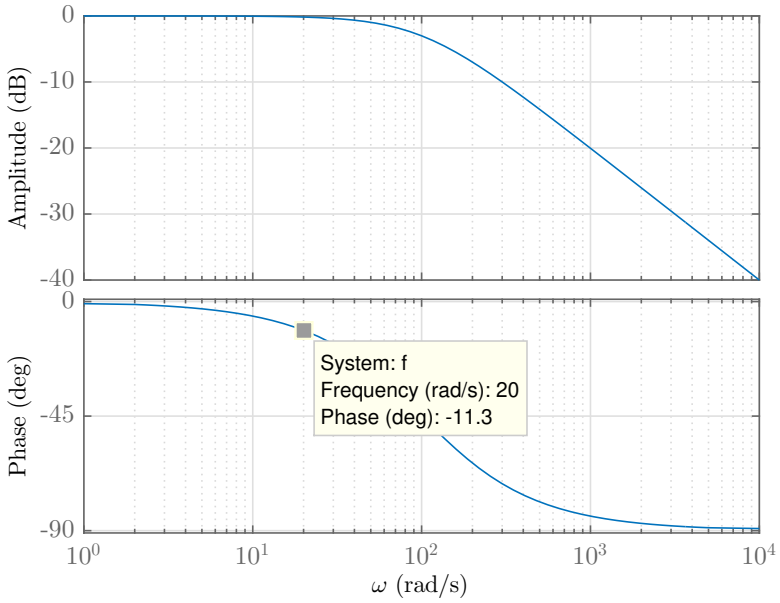

Figure 22 – Bode diagrams of the low-pass filter

4.3.5 Trade-offs

The Bode and Nyquist plots of the controlled system are given at figures 23 and 24. The different tradeoffs that had to be made are explicited in the different sections concerning

the components we have used. We had to make compromises for the phase margin, the rejection of noise and the use of a lag compensator.

Concerning the output and the controllable input (Figures 25 and 26, 27 and 28), we can see that the damping is very well obtained, although the force needed for the damper is a bit over what we have used in our constraints (not using a lag compensator brings us below them in the case of a constant wind but not in the case of a sinusoidal one). We have tried numerous changes in parameters to go below these constraints for the sinusoidal wind but have not succeeded.

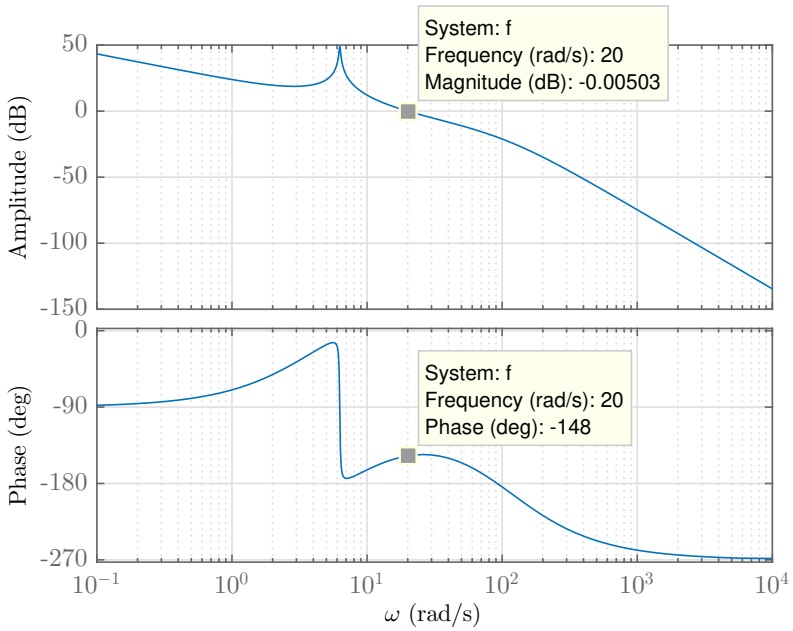

Figure 23 – Bode plots of the controlled system

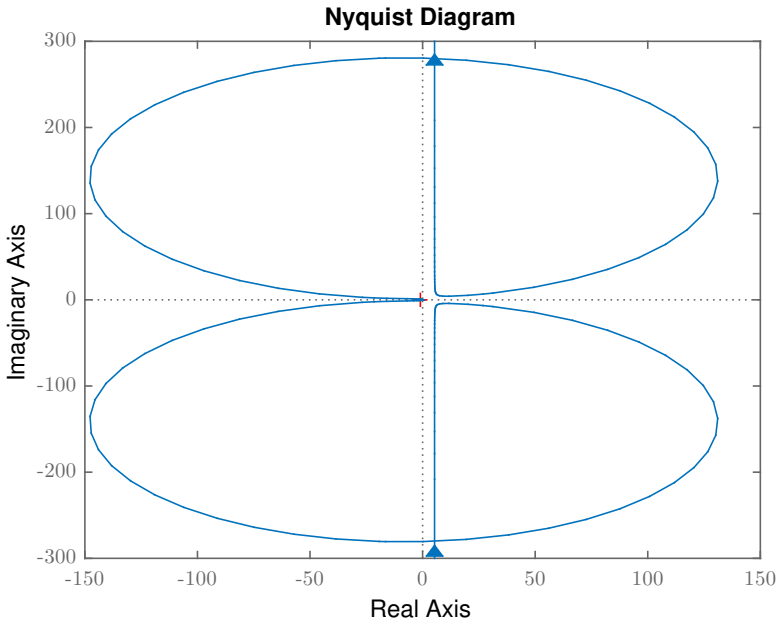

Figure 24 – Nyquist plot of the controlled system

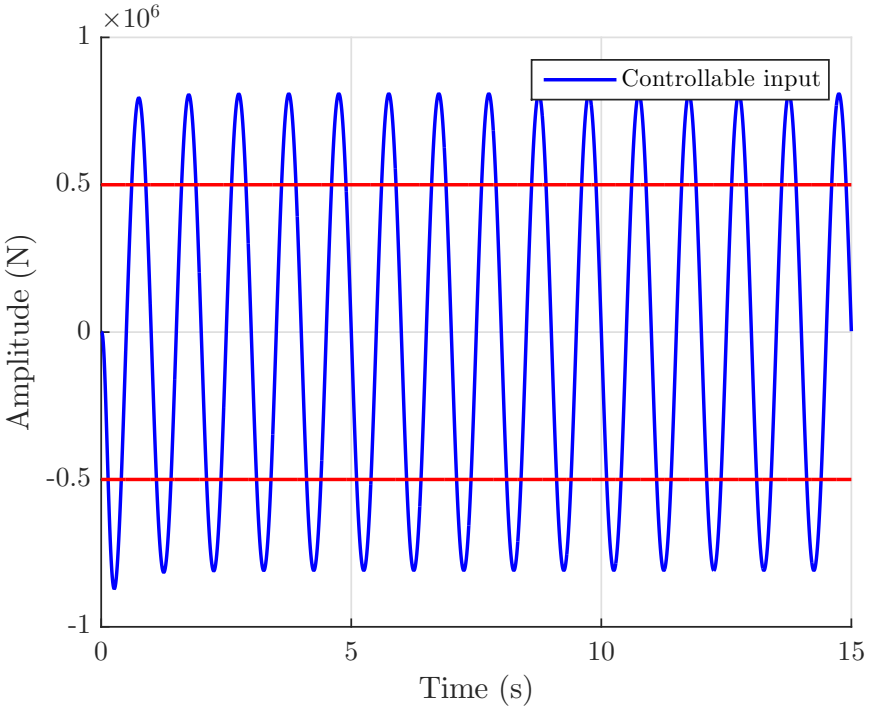

Figure 25 – Plot of the controllable input of the controlled system subjected to sinusoidal wind

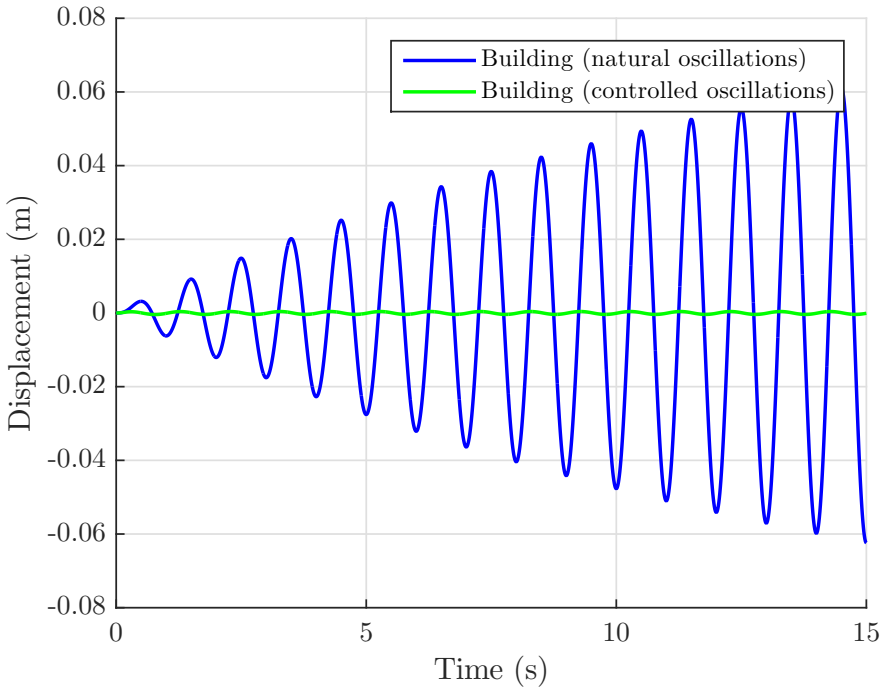

Figure 26 – Plot of the output of the controlled system subjected to sinusoidal wind

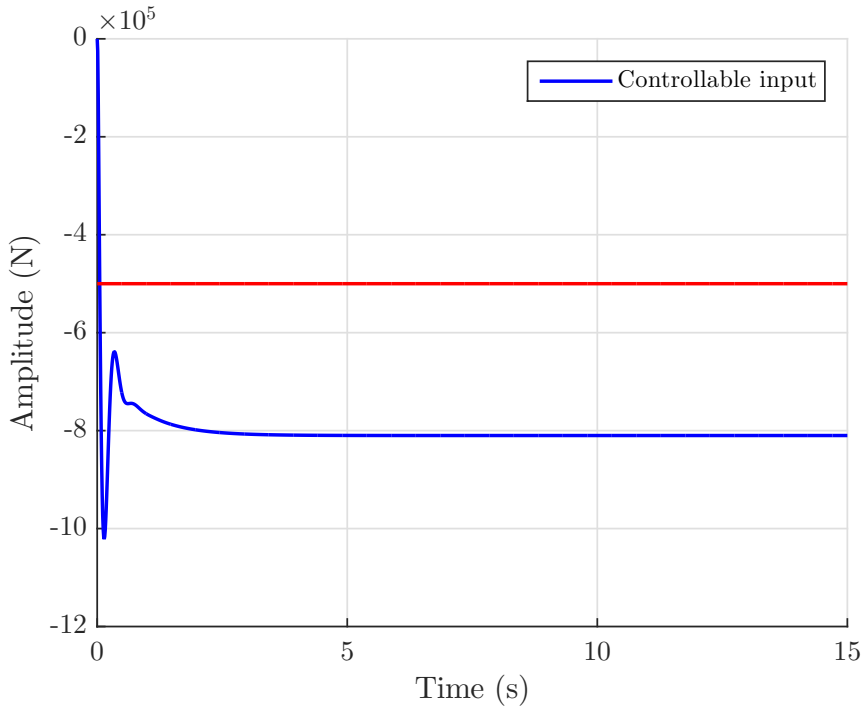

Figure 27 – Plot of the controllable input of the controlled system subjected to a constant wind

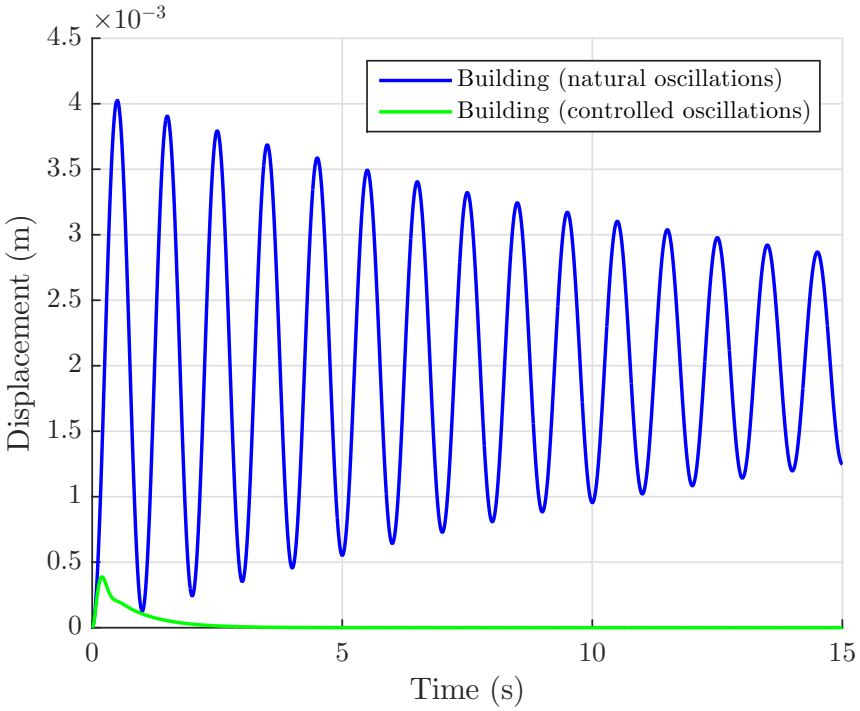

Figure 28 – Plot of the output of the controlled system subjected to a constant wind

4.4 Gang of four

4.4.1 Sensitivity function

$$S(s) = \frac{1}{1 + PC}$$

The Bode plots of the sensitivity function are given at figure 29. That function tells how the noise acts on the output. We do not want the system to react to the noise, as it is actually the measurement noise that must stay in the output.

As noise is a high-frequency phenomenon, we want to have no attenuation of high frequencies in the Bode plot of S. As can be seen, it is the case. We have a gain of 0dB for higher frequencies.

In the amplitude graph, we can see a small bump before stabilizing at $0dB$. That is the stability margin, which should remain small. It is not too high in our case, as the maximum sensitivity $M_s = 3.1dB$ and it occurs between 23 and 24 rad/s. As the stability margin is equal to the inverse of M_s, a high value for M_s would induce a small stability margin and larger amplifications of the disturbances.

Remark If we wanted a lower gain for lower frequencies (better resistance to disturbance), we would have a greater M_s as, due to Bode's integral formula, the integral of $\log(|S|)$ over R^+ is equal to 0 (waterbed effect).

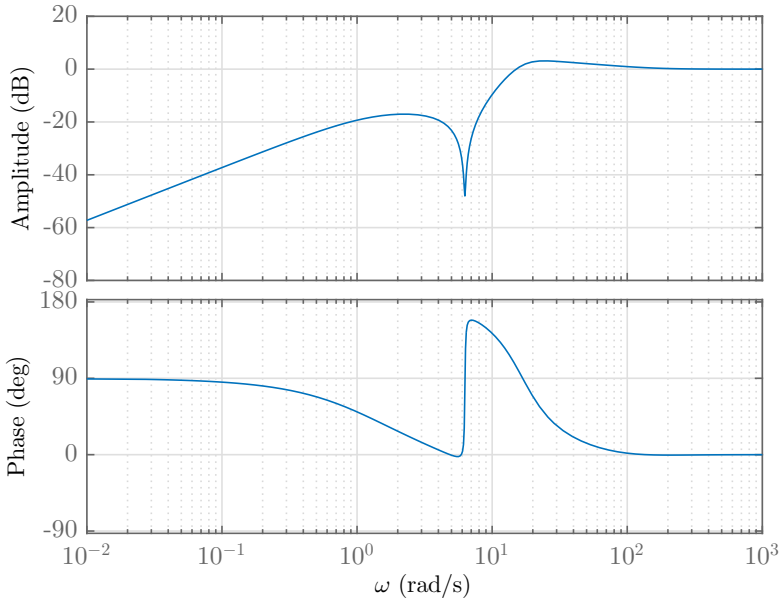

Figure 29 – Bode plots of the sensitivity function

4.4.2 Load sensitivity function

$$PS(s) = \frac{P}{1 + PC}$$

This function tells how the disturbances act on the output and the Bode diagrams are given at figure 30. The system needs to be robust against disturbances. In the present case, these disturbances are low frequency phenomena (frequency of the wind, which we have either chosen constant or a sine function of frequency equal to 1 Hz). We can see that we have a very good reaction concerning the effect of the wind on the output of the system (attenuation of about $-200\,\mathrm{dB}$).

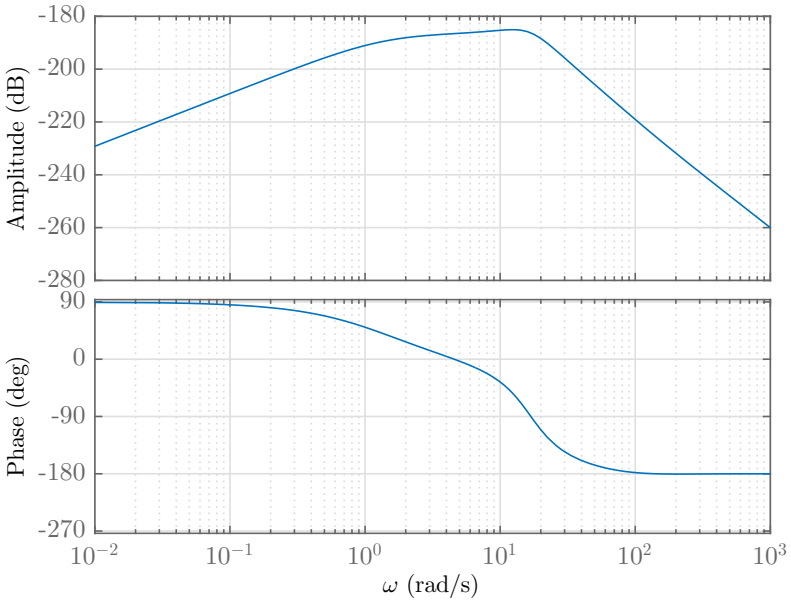

Figure 30 – Bode plots of the load sensitivity function

4.4.3 Complementary sensitivity function

$$T(s) = \frac{PC}{1 + PC}$$

This function tells us how the disturbances act on the controllable input and the reference acts on the output and the controllable input, and the Bode diagrams are given at figure 31.

The control signal must be reactive to disturbance and the output should be able to track the reference. Amplitudes at low frequency should therefore not be dampened, and one sees that they are not attenuated on the plots. After the maximum complementary sensitivity M_t, we have a decreasing slope in amplitude which makes it so that high frequency phenomena (such as noise) are attenuated. (As $S + T = 1$, we can see that we have a tradeoff between resistance to noise and resistance to disturbance. Better resistance to one induces a worse resistance to the other.)

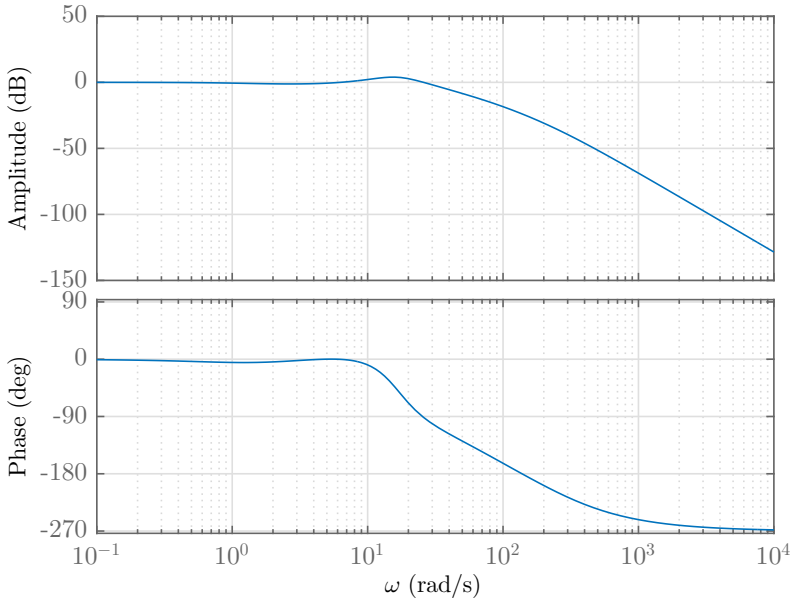

Figure 31 – Bode plots of the complementary sensitivity function

4.4.4 Noise sensitivity function

$$CS(s) = \frac{C}{1 + PC}$$

This function tells us how the noise and the reference act on the controllable input, and the Bode diagrams are given at figure 32.

That function should be reactive to reference changes, but not to noise, and so have a high magnitude at low frequency and low magnitude at high frequencies. One can see that it is not the case here. Indeed, one has high amplitudes for high frequencies. However, as our reference does not change in our system (we do not plan on dampening the oscillations in a Pisa Tower), it does not really matter.

It is also known that temporal domain controllers are better at reacting to reference changes than frequency domain ones.

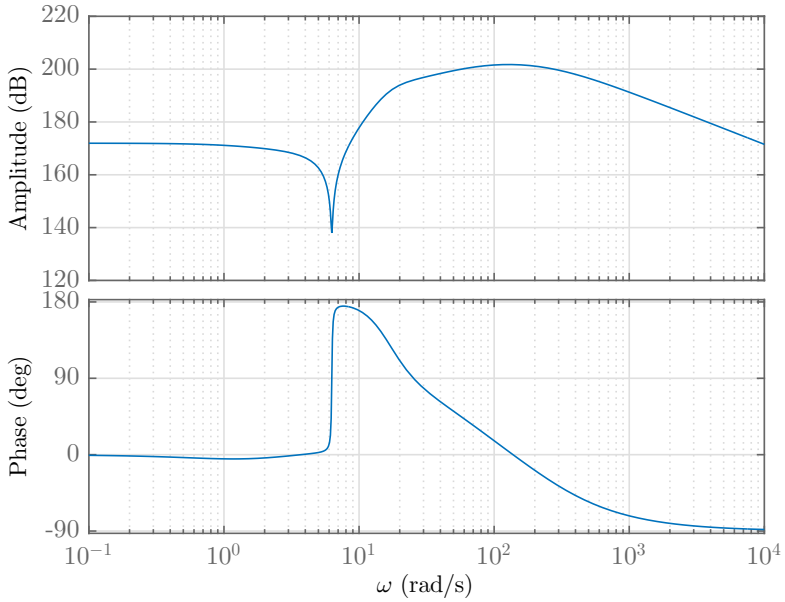

Figure 32 – Bode plots of the noise sensitivity function

4.5 Delays

The delays in our system are due to the sensor transmitting the information, the microcontroller processing that information and the actuator (piston) actually moving our mass damper. We have chosen that last source of delay as being the biggest one, with a frequency of 50 Hz, which induces delays of 0.02 s (discussed in the lead compensator).[]

Some Bode and Nyquist plots showing delays are given at figures 33, 34 and 35. It cannot be seen, but the curve for the delay of $0.02s$ on the Nyquist plot for the lowest phase encompasses the -1 value out of the image.

As can be seen, for a phase margin of 42°, the delays in our system do not bring instabilities. However, for larger delays, such as the $0.5s$ we have used to simulate Figure 36, we can clearly see some instabilities in our system. If we wanted to be resistant to such delays, we should increase the phase margin by placing our lag compensator and low-pass filter further away from the crossover frequency.

We decided to not include figures comparing the output and the controllable input in the case of delays or not because we ran out of space and we saw almost no difference. The two scenarios reached the same state with only a fraction of a second apart from one another. What happens when the delay is too big, however, is shown in Figure 36.

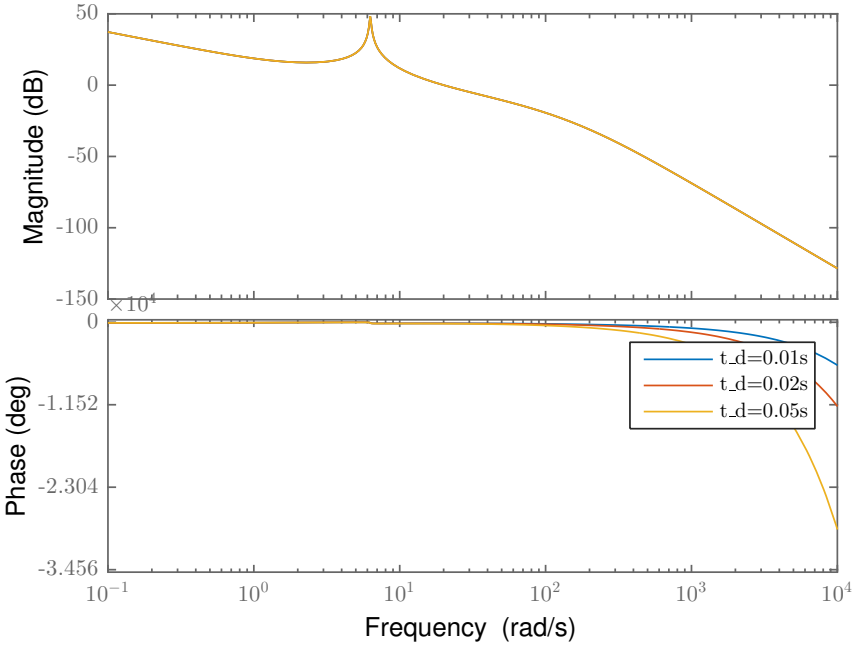

Figure 33 – Bode plots for various delays and a phase margin of 42 degrees

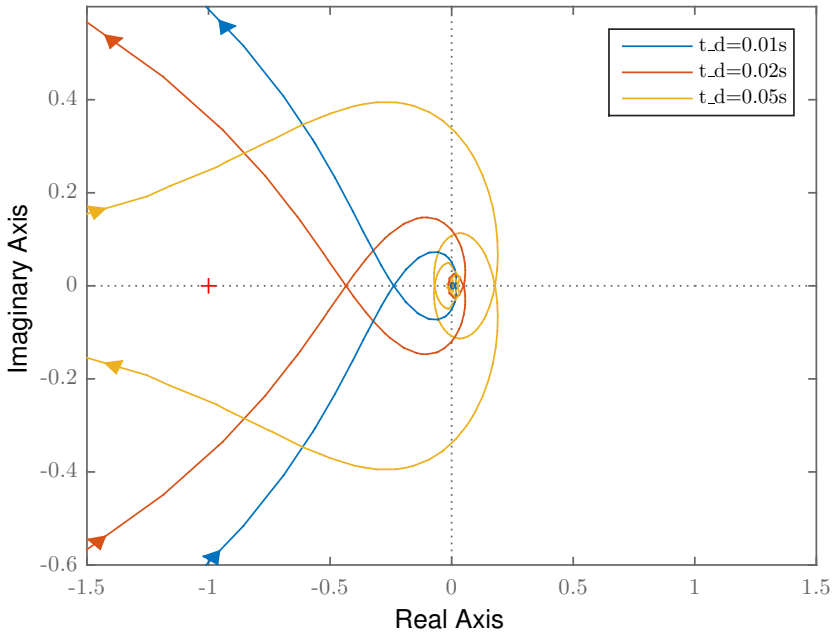

Figure 34 – Nyquist plots for various delays and a phase margin of 42 degree

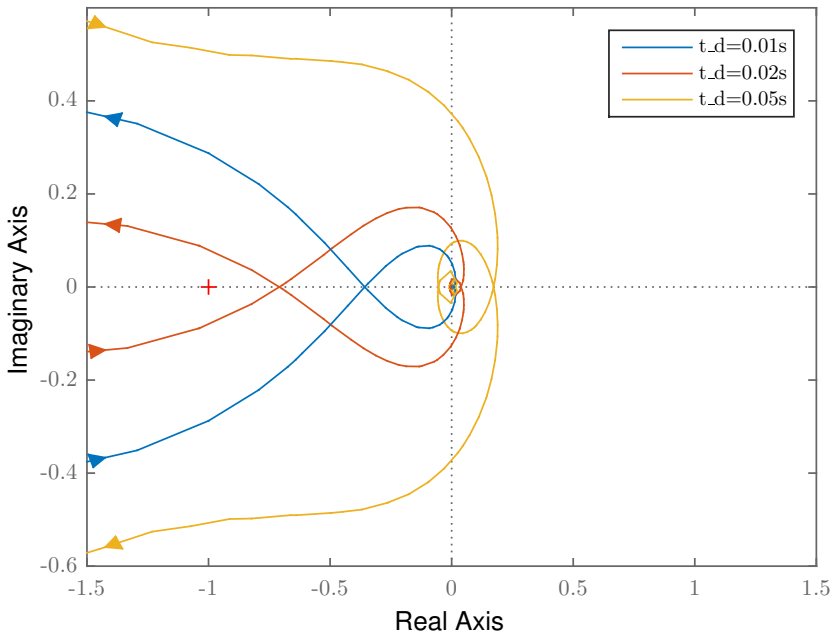

Figure 35 – Nyquist plots for various delays and a phase margin of 27 degrees

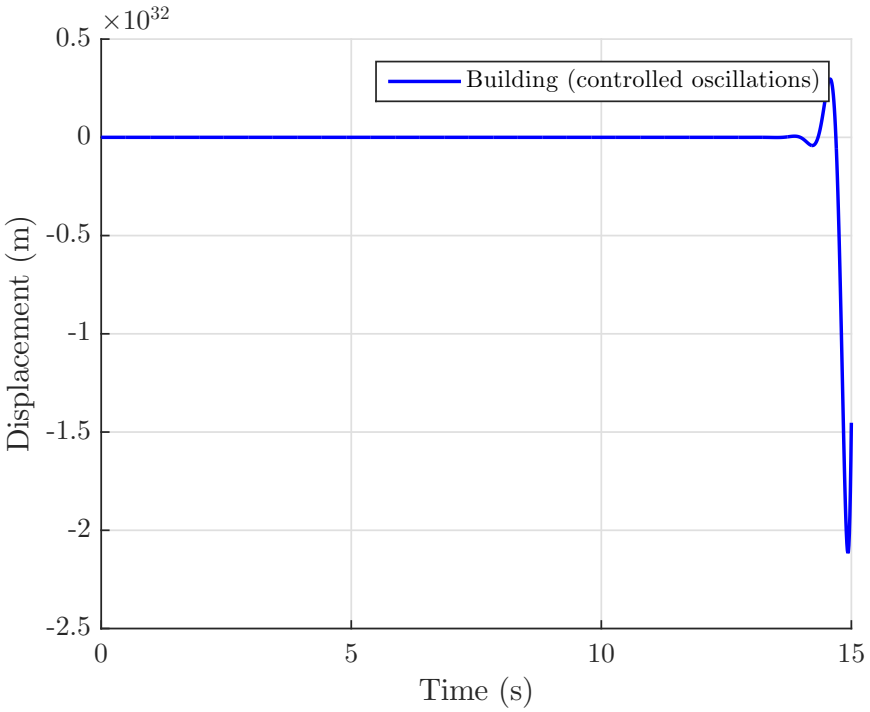

Figure 36 – Output of our controlled system with a delay of 0.5s

4.6 Noise

As we can see in Figures 37, 38 and 39, our system reacts quite well to noise thanks to our low-pass filter. Had we not implemented that filter, we can see that the effect on our controllable input is visible and prone to disturb our control. We did not plot the response of the building as it was not really influenced by noise, whether or not a low-pass filter is added.

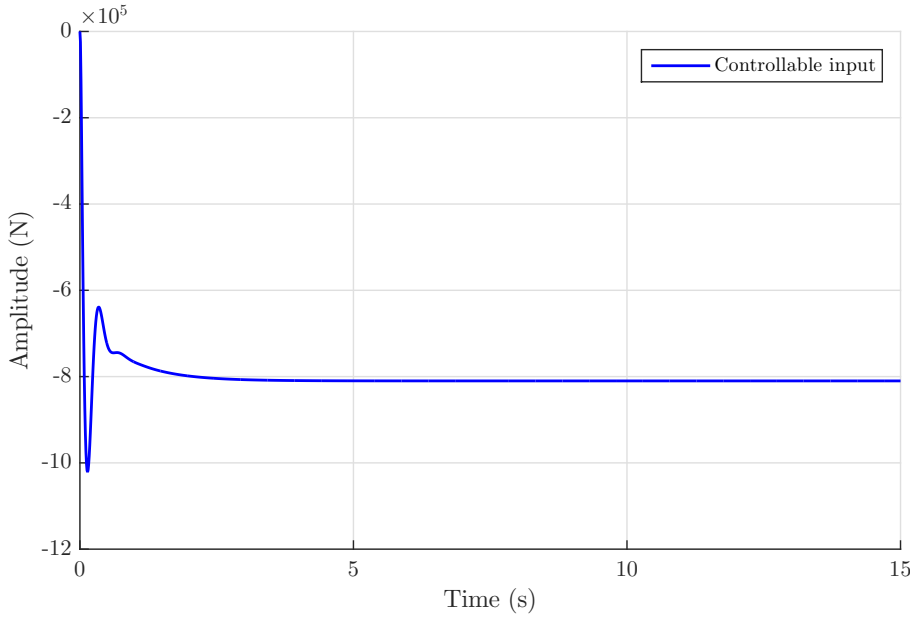

Figure 37 – Controllable input of our system with a constant wind and no noise

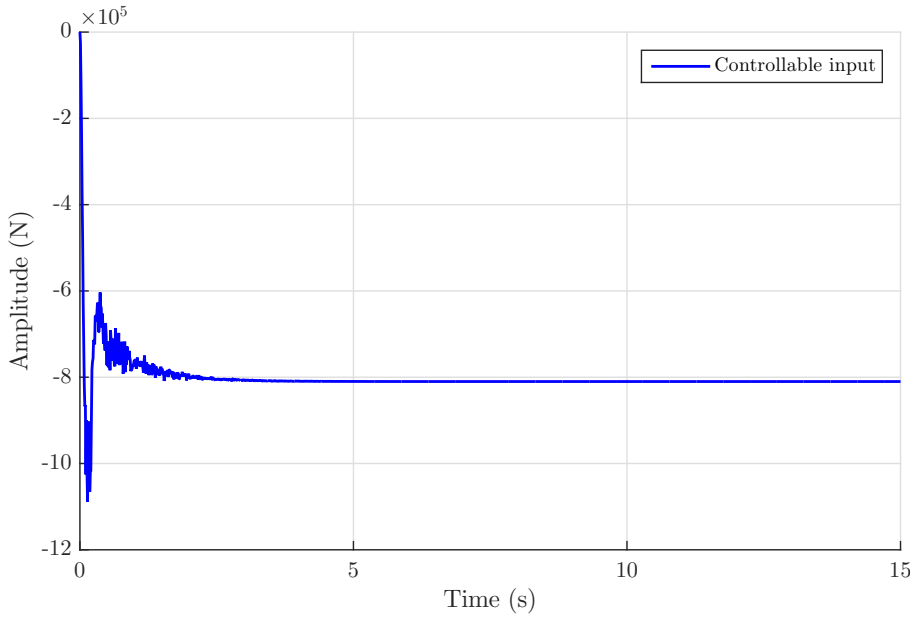

Figure 38 – Controllable input of our system with a constant wind, some noise and a low-pass filter

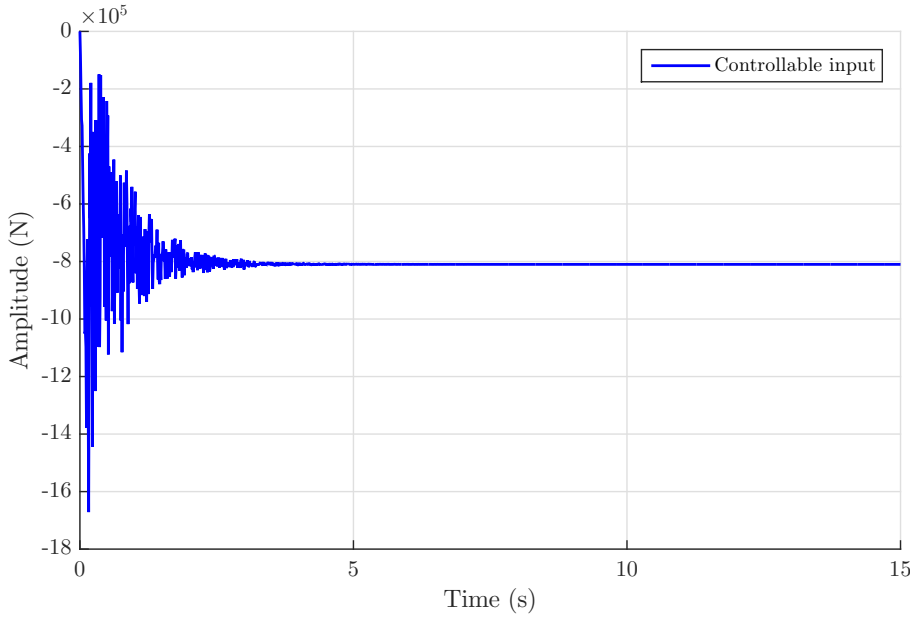

Figure 39 – Controllable input of our system with a constant wind, some noise and no low-pass filter

5 Conclusion

5.1 Time and frequency domains

The first thing we can observe when comparing the time and frequency controllers is that we do not have a **static error** in the frequency domain, thanks to the lag compensator. The **noise rejection** is quite good in both domains. In the time one, it may be explained by the fact that the observer acts as a filter. Indeed, the output of the system being one of the states it has to approximate on the basis of two non noisy inputs and a noisy one, the noise rejection is simplified. For the frequency domain, it is done thanks to the low-pass filter.

Concerning the reaction to a **reference change**, we found out that the frequency controller allowed us to reach that reference before $3s$, at the cost of an unbelievably high force applied on the damper. It is not plotted because we ran out of space and it was not asked explicitly, but we have a spike at $1.3m$ for the displacement of the building then a stabilization at 1m. It is not the case for the time domain, where we have huge displacements and no stabilization that we can observe in a reasonable time. That is counter-intuitive as we thought that a controller in time domain would track a reference better than one in frequency domain.

Concerning the **delays**, the frequency domain deals with them more easily than the time domain, although not by much. Indeed, as can be seen in Figure 40, the time controller is also quite good with small delays ($0.02s$).

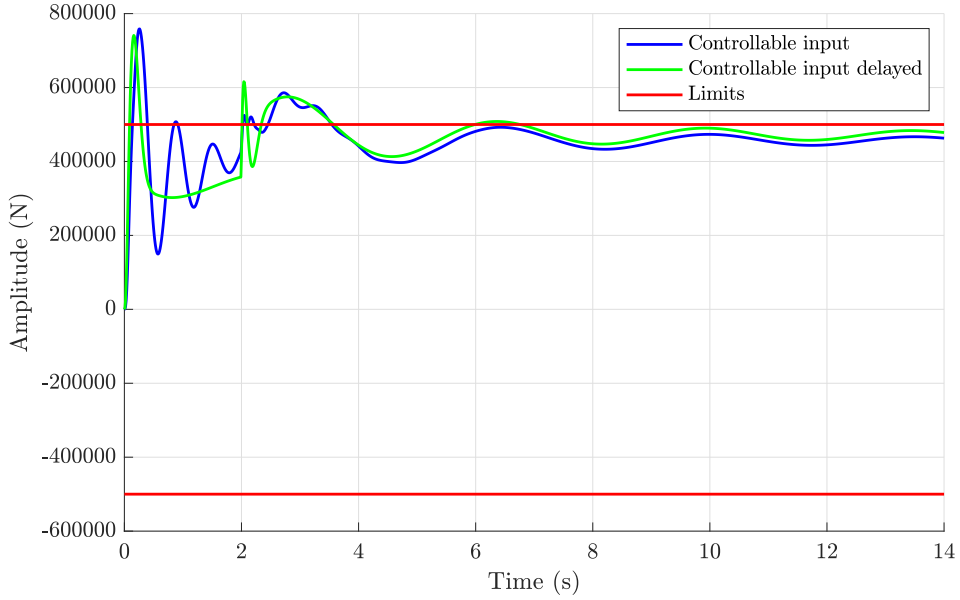

Figure 40 – Time controller simulation with 0.02s of delay.

5.2 General conclusion

This project allowed us to put in practice a lot of concepts that were explained in the theoretical lectures. However, we could not reach controllers that complied with the constraints Pr Denoël gave us (an acceleration between 0.3 and $0.6g$). This may come from the fact that some parameters had wrong values or that we oversimplified the problem.

We played with the different parameters of our controllers a huge amount of time in order to reach these constraints and the results presented in this report are the best we could manage. Using a bigger mass for the damper would have helped us reach our constraints, but we felt like 30 tons was already very heavy. We have thus decided to use an acceleration that was high, but not completely out of touch with reality. Although our results are not perfectly aligned with our initial constraint, we feel like we have understood the theoretical concepts we have applied, which was ultimately the goal of this project.

6 References

[1] *How To Stop Structures from SHAKING: LEGO Saturn V Tuned Mass Damper*. https://www.youtube.com/watch?v=ft3vTaYbkdE. Accessed : 2019-09-29.

[2] *Tuned mass damper*. https://en.wikipedia.org/wiki/Tuned_mass_damper. Accessed : 2019-09-29.

[3] Don-Ho Yang, Ji-Hwan Shin, HyunWook Lee, Seoug-Ki Kim, and Moon K. Kwak. "Active vibration control of structure by Active Mass Damper and Multi-Modal Negative Acceleration Feedback control algorithm". In: *Journal of Sound and Vibration* 392 (2017), pp. 18–30. ISSN: 0022-460X. DOI: https://doi.org/10.1016/j.jsv.2016.12.036. URL: http://www.sciencedirect.com/science/article/pii/S0022460X16307957.

[4] A Hassan, A Torres-Perez, S Kaczmarczyk, and P Picton. "The effect of time delay on control stability of an electromagnetic active tuned mass damper for vibration control". In: *Journal of Physics: Conference Series* 721 (May 2016), p. 012007. DOI: 10.1088/1742-6596/721/1/012007. URL: https://doi.org/10.1088%5C%2F1742-6596%5C%2F721%5C%2F1%5C%2F012007.

[5] Y.L. Xu. "Parametric study of active mass dampers for wind-excited tall buildings". In: *Engineering Structures* 18.1 (1996), pp. 64–76. ISSN: 0141-0296. DOI: https://doi.org/10.1016/0141-0296(95)00108-8. URL: http://www.sciencedirect.com/science/article/pii/0141029695001088.

[6] C C Chang, J F Wang, and C C Lin. "Parameter identification for active mass damper controlled systems". In: *Journal of Physics: Conference Series* 744 (Sept. 2016), p. 012166. DOI: 10.1088/1742-6596/744/1/012166. URL: https://doi.org/10.1088%5C%2F1742-6596%5C%2F744%5C%2F1%5C%2F012166.

[7] Student Handout. *Active Mass Damper - One Floor (AMD-1)*. https://www.made-for-science.com/de/quanser/?df=made-for-science-quanser-active-mass-damper-coursewarestud-matlab.pdf. Accessed : 2019-09-29.